Distribution functions in nonequilibrium theory of superconductivity and Andreev spectroscopy in unconventional superconductors

Matthias Eschrig*
Department of Physics & Astronomy, Northwestern University, Evanston, Illinois 60208
(Received 13 September 1999)

We develop a theoretical formulation of nonequilibrium superconducting phenomena, including singlet and triplet pairing, which is especially well suited for spatially inhomogeneous problems. We start from the general Keldysh-Nambu-Gor'kov Green's functions in the quasiclassical approximation and represent them in terms of 2×2 spin-matrix coherence functions and distribution functions for particle-type and hole-type excitations. The resulting transport equations for the distribution functions may be interpreted as a generalization to the superconducting state of Landau's transport equation for the normal Fermi liquid of conduction electrons. The equations are well suited for numerical simulations of dynamical phenomena. Using our formulation we solve an open problem in quasiclassical theory of superconductivity, the derivation of an explicit representation of Zaitsev's nonlinear boundary conditions (A. V. Zaitsev, Zh. Eksp. Teor. Fiz. **86**, 1742 (1984) [Sov. Phys. JETP **59**, 1015 (1984)]; A. L. Shelankov, Fiz. Tverd. Tela (Leningrad) **26**, 1615 (1984) [Sov. Phys. Solid State **26**, 981 (1984)]) at surfaces and interfaces. These boundary conditions include nonequilibrium phenomena and spin singlet and triplet unconventional pairing. We eliminate spurious solutions as well as numerical stability problems present in the original formulation. Finally, we formulate the Andreev scattering problem at interfaces in terms of the introduced distribution functions and present a theoretical analysis for the study of time reversal symmetry breaking states in unconventional superconductors via Andreev spectroscopy experiments at normal-metal–superconductor interfaces with finite transmission. We include impurity scattering self-consistently.

I. INTRODUCTION

Conduction electrons in normal metals are generally well described by Landau's Fermi liquid theory.[1] According to Landau a system of strongly interacting electrons may be viewed as an ensemble of quasiparticles which can be represented by a classical distribution function and obeys a semiclassical Landau-Boltzmann transport equation.[1] This semiclassical behavior of a quantum many-body system is a consequence of Pauli's exclusion principle which restricts the momentum space accessible to low-energy quasiparticles to a thin shell near the Fermi surface. The ratio of the volume of the accessible momentum space to the total volume enclosed by the Fermi surface is of the order $k_BT/E_f \ll 1$, and is the fundamental expansion parameter of Fermi liquid theory. Landau's Fermi liquid theory is exact in leading order in an asymptotic expansion in k_BT/E_F and other small parameters of an electronic Fermi liquid such as $1/k_f\xi_T$, $\hbar\omega/E_f$, $1/k_fl$, where E_f, k_f, ξ_T, ω, and l are Fermi energy, Fermi wave vector, thermal coherence length ($\xi_T=\hbar v_f/2\pi k_BT$), frequency of time-dependent perturbations, and quasiparticle mean free path. Phase space arguments can be used to derive Landau's Fermi liquid theory by converting a formal diagrammatic expansion of many-body Green's functions into an asymptotic expansion in the above small parameters.[2–4] Only a few of the resummed Feynman self-energy diagrams contribute in leading orders, and the dynamical equations for Green's functions can be transformed into Landau's transport equation for quasiparticle distribution functions.[5,6,2,3] The price one has to pay for the simplifications of the quasiparticle theory is the need to introduce phenomenological parameters, such as the quasiparticle velocities and quasiparticle interactions.[1,6] In the absence of first principles calculations these material parameters have to be taken from the experiment.

Eilenberger[7] and Larkin and Ovchinnikov[8] formulated the BCS pairing theory of superconductors[9] in equilibrium in terms of quasiclassical transport equations. This theory was generalized to nonequilibrium phenomena by Eliashberg[3] and Larkin and Ovchinnikov.[10] We regard this theory as the proper generalization of Landau's Fermi liquid theory to the superconducting state, and call this theory, following Larkin and Ovchinnikov,[8] the quasiclassical theory of superconductivity.

The derivation of the quasiclassical equations starts from Gor'kov's formulation of the theory of superconductivity in terms of Nambu-Gor'kov matrix Green's functions.[11] Gor'kov's Green's functions contain detailed information on atomic scale properties which average out on the superconducting scales. To derive the quasiclassical equations one has to integrate out atomic scale features in the Green's functions, but keep all relevant information for superconductivity. The resulting quasiclassical Green's functions vary on large scales such as the coherence length $\xi_0=\hbar v_f/2\pi k_BT_c$ and the time scale given by the inverse gap $t_0=\hbar/\Delta$, and are free of the irrelevant fine-scale structures. The quasiclassical equations should be compared with Andreev's equations[12] which he obtained by factorizing out rapidly oscillating terms in Bogoljubov's equations.[13,14] Andreev's method is equivalent to the quasiclassical theory for superconductors with infinitely long-lived quasiparticles, i.e., without impurities, electron-phonon coupling or electron-electron scattering. Both theories give identical results in these cases. Hence, the quasiclassical theory of Eilenberger, Larkin, Ovchinnikov, and Eliashberg may be considered a generali-

zation of Andreev's equations to systems with disorder and finite lifetimes of quasiparticles. The generalized theory covers basically all typical superconducting phenomena including Andreev's retroreflection,[12] Tomasch oscillations,[15] vortex bound states,[16] etc.

The complexity of dynamical phenomena in superconductors makes the elimination of atomic scale fine structure an important step towards a solution of dynamical problems. The dynamical equations of the quasiclassical theory can be formulated most compactly by using the Green's function technique of Keldysh.[17] It is often useful to distinguish two sources of time-dependent phenomena. First, time dependences can arise from changes in the occupation of quasiparticle states. In the normal phase of a Fermi liquid this is indeed the only fundamental dynamical process. Here, the quasiparticle states are robust and changes of the quasiparticle wave function can be neglected. This is no longer the case in the superconducting phase. Quasiparticle states in superconductors are coherent mixtures of particle and hole states determined by the superconducting order parameter. Since the order parameter will, in general, change in a dynamical process the quasiparticle states will also change. Superconducting dynamics is thus governed by the coupled dynamics of both the quasiparticle states and their occupation. The Keldysh technique is convenient in this case since it works with two types of Green's functions ($g^{R,A}$ and g^K) and can be used to introduce dynamical spectral functions describing the time development of quasiparticle states and dynamical distribution functions describing the time-dependent occupation of the states. Dynamical distribution functions in the superconducting state were introduced by Larkin and Ovchinnikov[10] and by Shelankov.[18]

In this paper we present an exact parametrization of the quasiclassical Keldysh Green's functions in terms of four coherence functions and two distribution functions. The coherence functions are generalizations of the Riccati amplitudes introduced recently[19,20] for superconductors in equilibrium, whereas the distribution functions are the generalizations of the distribution function of Landau's Fermi liquid theory of the normal state. Compared to the conventional quasiclassical theory our formulation leads to intuitively appealing and *explicit* boundary conditions at surfaces and interfaces, is numerically very stable, and allows for a more transparent interpretation of quasiclassical dynamics in terms of particle-type and hole-type excitations.

The general framework of the quasiclassical theory is briefly reviewed in Secs. II, III, where we also introduce our notation. Dynamical equations for the coherence functions are derived in Sec. IV together with dynamical equations for the distribution functions (transport equations). In Sec. V we solve Zaitsev's nonlinear boundary conditions for quasiclassical Green's functions at interfaces, and obtain physically appealing boundary conditions for our coherence functions and distribution functions. In Sec. VI we present the general linear response equations in terms of the introduced functions. Finally, we formulate in Sec. VII the Andreev scattering problem at interfaces between a normal metal and an unconventional superconductor using our theoretical formulation and the resulting boundary conditions. We present results for the Andreev reflection amplitudes and the regularly reflected amplitudes at (110) interfaces and (100) interfaces between a normal metal and a layered *d*-wave superconductor. Our formulation generalizes earlier work[21,22] to include disorder. We propose an anomalous feature in the reflection amplitudes for (110) interfaces as a test for time reversal symmetry breaking states. This feature, a strong suppression of the regular reflection for low-energy quasiparticles at interfaces with finite transmission, is sensitive to sign changes in the order parameter, and has the same origin as the zero-energy surface bound states. Combined with this suppression is an enhancement of the excess current due to Andreev reflection for low energy quasiparticles. The sensitivity of this phenomenon to time reversal symmetry breaking states provides an additional tool to study the symmetry of the order parameter. We study the effect of disorder on both regularly and Andreev reflected currents. For Andreev spectroscopy in unconventional superconductors the low-energy behavior of regular reflection is the spectral feature most stable against disorder.

II. KELDYSH SPACE STRUCTURE

The fundamental quantity in nonequilibrium quasiclassical theory of superconductivity is the quasiclassical Green's function $\check{g}=\check{g}(\mathbf{p}_f,\mathbf{R},\epsilon,t)$.[4,23,24] It is a 2×2 Keldysh matrix[17] of the form

$$\check{g}=\begin{pmatrix}\hat{g}^R & \hat{g}^K\\ \hat{0} & \hat{g}^A\end{pmatrix}, \tag{1}$$

where the elements are 4×4-Nambu-Gor'kov matrices, which describe the two important residual quantum mechanical (internal) degrees of freedom: the spin degree of freedom and the particle-hole degree of freedom. $\hat{g}^R=\hat{g}^R(\mathbf{p}_f,\mathbf{R},\epsilon,t)$ is the retarded, $\hat{g}^A=\hat{g}^A(\mathbf{p}_f,\mathbf{R},\epsilon,t)$ the advanced, and $\hat{g}^K=\hat{g}^K(\mathbf{p}_f,\mathbf{R},\epsilon,t)$ the Keldysh Green's function. The classical (external) degrees of freedom are described by a motion of the quasiparticles along classical trajectories. All trajectories through a spatial point $\mathbf{R}$ are parametrized by the Fermi momentum $\mathbf{p}_f$ and their directions coincide with the directions of the Fermi velocities $\mathbf{v}_f(\mathbf{p}_f)$. Along a given trajectory with fixed $\mathbf{p}_f$ all quasiparticles travel with the same velocity $\mathbf{v}_f(\mathbf{p}_f)$. In general there can be several branches of quasiparticles moving with the same velocity but having different momenta. Also the directions of $\mathbf{p}_f$ and $\mathbf{v}_f(\mathbf{p}_f)$ are generally different. However, for spherical or cylindrical Fermi surfaces $\mathbf{p}_f$ and $\mathbf{v}_f(\mathbf{p}_f)$ differ only by a scaling factor. The remaining parameters are the energy ϵ (measured from the chemical potential) and the time t.

The quasiclassical Green's function is solution of the following transport equation along a given trajectory, and of the corresponding normalization condition[3,7,8,10] (the $\otimes$ product is noncommutative and is explained in Appendix A)

$$[\check{\epsilon}-\check{h},\check{g}]_\otimes+i\hbar\mathbf{v}_f\nabla\check{g}=\check{0},\quad \check{g}\otimes\check{g}=-\pi^2\check{1}. \tag{2}$$

Here $\check{\epsilon}=\epsilon\hat{\tau}_3\check{1}$ represents the energy variable and $\check{h}$ combines the molecular (or mean) field self-energies $\check{\sigma}_{\mathrm{MF}}=\hat{\sigma}_{\mathrm{MF}}\check{1}$, the impurity and electron-phonon self-energies $\check{\sigma}_i$, and external potentials, $\check{v}_{\mathrm{ext}}=\hat{v}_{\mathrm{ext}}\check{1}$

$$\check{h}=\check{\sigma}_{\rm MF}+\check{\sigma}_i+\check{v}_{\rm ext}=\begin{pmatrix}\hat{h}^R & \hat{h}^K\\ \hat{0} & \hat{h}^A\end{pmatrix}. \tag{3}$$

Disorder will be included by following standard averaging procedure for dilute impurity concentrations.[25] We denote impurity self-energies by $\check{\sigma}_{\rm imp}$. In quasiclassical approximation ($l\gg 1/k_f$), the impurity self-energy can be written in terms of the concentrations c_i of impurities of type i and the single impurity t matrices $\check{t}_i$

$$\check{\sigma}_{\rm imp}(\mathbf{p}_f,\mathbf{R},\epsilon,t)=\sum_{i=1}^{N} c_i\check{t}_i(\mathbf{p}_f,\mathbf{p}_f;\mathbf{R},\epsilon,t). \tag{4}$$

The t matrices are solutions of the following equations (we suppress the variables $\mathbf{R},\epsilon,t$ for convenience):

$$\check{t}_i(\mathbf{p}_f,\mathbf{p}_f')=\check{u}_i(\mathbf{p}_f,\mathbf{p}_f') + N_f\langle\check{u}_i(\mathbf{p}_f,\mathbf{p}_f'')\otimes\check{g}(\mathbf{p}_f'')\otimes\check{t}_i(\mathbf{p}_f'',\mathbf{p}_f')\rangle_{\mathbf{p}_f''}, \tag{5}$$

where $\check{u}_i(\mathbf{p}_f,\mathbf{p}_f'')$ is the scattering potential of an impurity of type i. The Fermi surface average $\langle\cdots\rangle_{\mathbf{p}_f''}$ is explained in Appendix A. The impurity potential is diagonal in Keldysh space.

III. NAMBU-GOR'KOV SPACE STRUCTURE

In a standard notation of quasiclassical theory[4,23,24] the distribution functions are 4×4 matrices which reflects their quantum mechanical structure as density matrices in the four-dimensional Hilbert space of internal degrees of freedom (Nambu-Gor'kov space). We parametrize the elements of the Nambu matrices in the following way:

$$\hat{g}^{R,A}=\begin{pmatrix}g^{R,A} & f^{R,A}\\ \tilde{f}^{R,A} & \tilde{g}^{R,A}\end{pmatrix},\quad \hat{g}^{K}=\begin{pmatrix}g^{K} & f^{K}\\ -\tilde{f}^{K} & -\tilde{g}^{K}\end{pmatrix}, \tag{6}$$

$$\hat{h}^{R,A}=\begin{pmatrix}\Sigma^{R,A} & \Delta^{R,A}\\ \tilde{\Delta}^{R,A} & \tilde{\Sigma}^{R,A}\end{pmatrix},\quad \hat{h}^{K}=\begin{pmatrix}\Sigma^{K} & \Delta^{K}\\ -\tilde{\Delta}^{K} & -\tilde{\Sigma}^{K}\end{pmatrix}. \tag{7}$$

Here $g^{R,A}$, $\tilde{f}^{R,A}$, Δ^K, etc. are 2×2 spin matrices.

The molecular fields are determined by Landau's quasiparticle interaction function $A(\mathbf{p}_f,\mathbf{p}_f')$, leading to a self-energy spin matrix $\hat{\nu}_{mf}(\mathbf{p}_f,\mathbf{R},\epsilon,t)$, which is diagonal in particle-hole space. In superconductors this interaction must be supplemented by the pairing interaction of quasiparticles $V(\mathbf{p}_f,\mathbf{p}_f')$ which lead to an off-diagonal self-energy in particle-hole space $\hat{\Delta}_{mf}(\mathbf{p}_f,\mathbf{R},\epsilon,t)$. Thus,

$$\hat{\sigma}_{\rm MF}=\hat{\nu}_{\rm MF}+\hat{\Delta}_{\rm MF}. \tag{8}$$

The mean-field self energies, Eq. (8), are diagonal in Keldysh space.[4] Their matrix structure in Nambu space is

$$\hat{\Delta}_{\rm MF}=\begin{pmatrix}0 & \Delta_{\rm MF}\\ \tilde{\Delta}_{\rm MF} & 0\end{pmatrix},\hat{\nu}_{\rm MF}=\begin{pmatrix}\nu_{\rm MF} & 0\\ 0 & \tilde{\nu}_{\rm MF}\end{pmatrix}. \tag{9}$$

Not all the matrix elements are independent from each other, but are related by symmetry relations.[4] For instance, a quantity q and the conjugated quantity $\tilde{q}$ are related by

$$\tilde{q}(\mathbf{p}_f,\mathbf{R},\epsilon,t)=q(-\mathbf{p}_f,\mathbf{R},-\epsilon,t)^*. \tag{10}$$

The conjugation operator $(\tilde{\ })$ defines an important transformation of quasiclassical Green's functions and self-energies. We will use it extensively in the following.

IV. COHERENCE FUNCTIONS AND DISTRIBUTION FUNCTIONS

The numerical solution of the transport equations for the quasiclassical Green's functions can be simplified considerably by introducing a special parametrization in terms of 2×2 spin matrix coherence functions $\gamma^{R,A}$, $\tilde{\gamma}^{R,A}$, and distribution functions x^K and $\tilde{x}^K$, which transforms the original boundary value problem for $\check{g}$ into initial value problems for the coherence and distribution spin matrices. The normalization condition is eliminated completely in this formulation. We present here the resulting equations and refer for their derivation to Appendixes B and C. Before doing this we give a short physical interpretation for the coherence functions. In the absence of particle-hole coherence, as in the equilibrium normal state, the functions $\gamma^{R,A}$, $\tilde{\gamma}^{R,A}$ vanish. A superconductor, or a normal metal in proximity to a superconductor, can be described in equilibrium and in the clean limit by Andreev's equations[12] with Andreev amplitudes u and v. Then, the coherence function γ^R, for example, is given in terms of the u- and v-spin matrices (for positive energies) by the solution of the linear system $\Sigma_\beta u_{\alpha\beta}\gamma^R_{\beta\delta}=v_{\alpha\delta}$. Thus, the coherence functions are the transformation matrices between the particlelike and holelike Andreev amplitudes. In the presence of quasiparticle damping the Andreev description breaks down, nevertheless one can *define* generalized amplitudes $u^{R,A}$ and $v^{R,A}$. In nonequlilbrium they are defined by relations such as $u^R\otimes\gamma^R=v^R$. Note that these generalized amplitudes are defined by the quasiclassical Green's functions, not by wave functions.

The quasiclassical Green's functions are conveniently parametrized by

$$\hat{g}^{R,A}=\mp i\pi \times\hat{N}^{R,A}\otimes\begin{pmatrix}(1+\gamma^{R,A}\otimes\tilde{\gamma}^{R,A}) & 2\gamma^{R,A}\\ -2\tilde{\gamma}^{R,A} & -(1+\tilde{\gamma}^{R,A}\otimes\gamma^{R,A})\end{pmatrix}, \tag{11}$$

$$\hat{g}^{K}=-2\pi i \times\hat{N}^{R}\otimes\begin{pmatrix}(x^K-\gamma^R\otimes\tilde{x}^K\otimes\tilde{\gamma}^A) & -(\gamma^R\otimes\tilde{x}^K-x^K\otimes\gamma^A)\\ -(\tilde{\gamma}^R\otimes x^K-\tilde{x}^K\otimes\tilde{\gamma}^A) & (\tilde{x}^K-\tilde{\gamma}^R\otimes x^K\otimes\gamma^A)\end{pmatrix} \otimes\hat{N}^{A}, \tag{12}$$

with the ''normalization matrices''

$$\hat{N}^{R,A}=\begin{pmatrix}(1-\gamma^{R,A}\otimes\tilde{\gamma}^{R,A})^{-1} & 0\\ 0 & (1-\tilde{\gamma}^{R,A}\otimes\gamma^{R,A})^{-1}\end{pmatrix}. \tag{13}$$

In Eq. (11) the factor $\hat{N}^{R,A}$ may be written on the left- or right-hand side. The transport equations for the 2×2 spin matrix functions are

$$i\hbar\mathbf{v}_f\nabla\gamma^{R,A}+2\epsilon\gamma^{R,A} = \gamma^{R,A}\otimes\tilde{\Delta}^{R,A}\otimes\gamma^{R,A}+\Sigma^{R,A}\otimes\gamma^{R,A}-\gamma^{R,A}\otimes\tilde{\Sigma}^{R,A}-\Delta^{R,A}, \tag{14}$$

$$i\hbar\mathbf{v}_f\nabla\tilde{\gamma}^{R,A}-2\epsilon\tilde{\gamma}^{R,A} = \tilde{\gamma}^{R,A}\otimes\Delta^{R,A}\otimes\tilde{\gamma}^{R,A}+\tilde{\Sigma}^{R,A}\otimes\tilde{\gamma}^{R,A}-\tilde{\gamma}^{R,A}\otimes\Sigma^{R,A}-\tilde{\Delta}^{R,A}, \tag{15}$$

$$i\hbar\mathbf{v}_f\nabla x^K+i\hbar\partial_t x^K +(-\gamma^R\otimes\tilde{\Delta}^R-\Sigma^R)\otimes x^K+x^K\otimes(-\Delta^A\otimes\tilde{\gamma}^A+\Sigma^A) = -\gamma^R\otimes\tilde{\Sigma}^K\otimes\tilde{\gamma}^A+\Delta^K\otimes\tilde{\gamma}^A+\gamma^R\otimes\tilde{\Delta}^K-\Sigma^K, \tag{16}$$

$$i\hbar\mathbf{v}_f\nabla\tilde{x}^K-i\hbar\partial_t\tilde{x}^K +(-\tilde{\gamma}^R\otimes\Delta^R-\tilde{\Sigma}^R)\otimes\tilde{x}^K+\tilde{x}^K\otimes(-\tilde{\Delta}^A\otimes\gamma^A+\tilde{\Sigma}^A) = -\tilde{\gamma}^R\otimes\Sigma^K\otimes\gamma^A+\tilde{\Delta}^K\otimes\gamma^A+\tilde{\gamma}^R\otimes\Delta^K-\tilde{\Sigma}^K. \tag{17}$$

Equations (11), (14), and (15) generalize a useful formulation of the equilibrium theory in terms of Riccati-type transport equations[19,20] to nonequilibrium phenomena. Equations (11)–(17) are[26] numerically very stable and provide an efficient way to solve nonequilibrium problems in superconductors. Equations (14)–(17) need to be supplemented by initial conditions. They are imposed for γ^R, $\tilde{\gamma}^A$, and x^K at the beginning of the trajectory, and for γ^A, $\tilde{\gamma}^R$, and $\tilde{x}^K$ at the end of the trajectory. For correctly chosen initial conditions the transport equations for γ^R, $\tilde{\gamma}^A$, and x^K are stable in positive $\mathbf{v}_f$ direction, and the transport equations for γ^A, $\tilde{\gamma}^R$, and $\tilde{x}^K$ are stable in negative $\mathbf{v}_f$ direction. In addition to the conjugation symmetries the coherence and distribution functions obey the following symmetries

$$\gamma^A(\mathbf{p}_f,\mathbf{R},\epsilon,t)=\tilde{\gamma}^R(\mathbf{p}_f,\mathbf{R},\epsilon,t)^\dagger, \tag{18}$$

$$x^K(\mathbf{p}_f,\mathbf{R},\epsilon,t)=x^K(\mathbf{p}_f,\mathbf{R},\epsilon,t)^\dagger. \tag{19}$$

Note that the $x^K(\mathbf{p}_f,\mathbf{R},\epsilon,t)$, $\tilde{x}^K(\mathbf{p}_f,\mathbf{R},\epsilon,t)$ are Hermitean spin matrices. In equilibrium,

$$x^K_{\rm eq}=(1-\gamma^R\tilde{\gamma}^A)\tanh\frac{\epsilon}{2T}. \tag{20}$$

There is no unique definition of quasiclassical distribution functions for superconductors. Various different but physically equivalent distribution functions have been introduced.[10,23,24,18,27–30] Our distribution functions x^K and $\tilde{x}^K$ are similar to the distribution functions of Shelankov.[18] The relation between Shelankov's distribution functions and our's is given in Eq. (C11). These distribution functions have the direct physical interpretation in terms of particle-type and hole-type excitations, i.e., excitations whose velocity is along and opposite to their momentum.

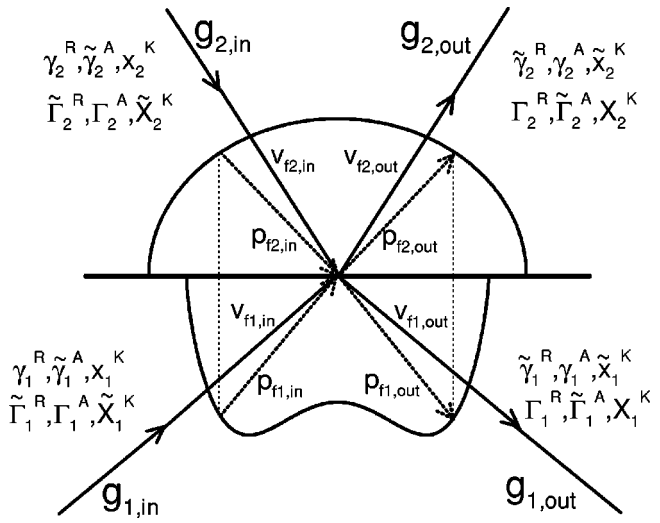

FIG. 1. Notation for the Green's functions at the interface. Indices 1 and 2 refer to the sides of the interface. The arrows for the Fermi momenta (dotted) are for particlelike excitations. The Fermi velocity directions (full lines) are given by the directions perpendicular to the Fermi surface (full curves) at the corresponding Fermi momentum. The components of the Fermi momenta parallel to the surface are conserved (indicated by the thin dotted lines).

V. EXPLICIT SOLUTION OF ZAITSEV'S NONLINEAR BOUNDARY CONDITIONS

In the previous sections we have introduced a parametrization of the nonequilibrium Keldysh Green's function $\check{g}$ in terms of four coherence functions and two distribution functions (2×2 spin matrices)

$$\check{g}=\check{g}[\gamma^R,\tilde{\gamma}^R,\gamma^A,\tilde{\gamma}^A,x^K,\tilde{x}^K]. \tag{21}$$

An important problem is the formulation of boundary conditions for these parameters at surfaces and interfaces.[31–36] A boundary condition for $\check{g}$ was obtained by Zaitsev,[31] which in principle solves this problem for perfect interfaces. However, Zaitsev's nonlinear boundary conditions have unphysical spurious solutions which require special care, e.g., in a numerical implementation. A linearization of Zaitsev's boundary conditions for the equilibrium was achieved recently by Yip[36] for the case of an interface connected to infinite half spaces. Our solution generalizes these results to any interface geometry and to nonequilibrium phenomena. Zaitsev's condition relates the quasiclassical Green's functions with Fermi velocity pointing in direction towards the surface $\check{g}_{1,\rm in}$, $\check{g}_{2,\rm in}$, and those with Fermi velocity pointing away $\check{g}_{1,\rm out}$, $\check{g}_{2,\rm out}$. Indices 1 and 2 refer to the two sides of the interface (see Fig. 1). Using the definitions

$$\check{P}_1=\frac{i}{2\pi}(\check{g}_{1,\rm in}+\check{g}_{1,\rm out}),\quad \check{P}_2=\frac{i}{2\pi}(\check{g}_{2,\rm in}+\check{g}_{2,\rm out}), \tag{22}$$

$$\check{P}_a=\frac{i}{2\pi}(\check{g}_{1,\rm in}-\check{g}_{1,\rm out})=\frac{i}{2\pi}(\check{g}_{2,\rm out}-\check{g}_{2,\rm in}), \tag{23}$$

which fulfill the relations

$$\check{P}_a\otimes\check{P}_1+\check{P}_1\otimes\check{P}_a=\check{0},\quad \check{P}_a\otimes\check{P}_a+\check{P}_1\otimes\check{P}_1=\check{1}, \tag{24}$$

$$\check{P}_a\otimes\check{P}_2+\check{P}_2\otimes\check{P}_a=\check{0},\quad \check{P}_a\otimes\check{P}_a+\check{P}_2\otimes\check{P}_2=\check{1},\quad (25)$$

Zaitsev's boundary conditions read[31]

$$[(\check{1}-\check{P}_a)\otimes\check{P}_1\otimes\check{P}_2-(\check{1}+\check{P}_a)\otimes\check{P}_2\otimes\check{P}_1](1-\mathcal{R})$$
$$=-2\check{P}_a\otimes(\check{1}-\check{P}_a\otimes\check{P}_a)(1+\mathcal{R}).\quad (26)$$

Here, and in the following $\mathcal{R}=\mathcal{R}(\mathbf{p}_f)$ and $\mathcal{D}=\mathcal{D}(\mathbf{p}_f)$ are the reflection and transmission coefficients of the interface for quasiparticles in the normal state correspondingly, $\mathcal{R}(\mathbf{p}_f)+\mathcal{D}(\mathbf{p}_f)=1$. In the following we present the explicit solution of Zaitsev's nonlinear boundary conditions at spin-conserving interfaces in terms of the coherence functions and distribution functions introduced above. It is useful for this purpose to introduce a notation which indicates the stability properties of solutions of the transport equations. We use capital letters ($\Gamma^{R,A},\tilde{\Gamma}^{R,A},X^K,\tilde{X}^K$) for functions, which are stable solutions when integrating the transport equation towards the surface. Small case letters ($\gamma^{R,A},\tilde{\gamma}^{R,A},x^K,\tilde{x}^K$) are used for functions, which are stable in the direction away from the surface. We also generalize the notation for the conjugation operation. It includes a conversion from small case to capital case letters

$$\tilde{q}(\mathbf{p}_f,\mathbf{R},\epsilon,t)=Q(-\mathbf{p}_f,\mathbf{R},-\epsilon,t)^*\quad (27)$$

and vice versa. By integrating in direction towards the surface, the quantities $\gamma_j^{R,A},\tilde{\gamma}_j^{R,A},x_j^K,\tilde{x}_j^K$ $(j=1,2)$ are known. The quantities $\Gamma_j^{R,A},\tilde{\Gamma}_j^{R,A},X_j^K,\tilde{X}_j^K$ are to be determined by integrating in direction away from the surface. At the surface the second set of quantities is determined in terms of the first one by boundary conditions.

The incoming quasiclassical retarded Green's functions (with velocity direction towards the interface) on each side of the interface are given then by (see Fig. 1)

$$\check{g}_{1,\mathrm{in}}=\check{g}[\gamma_1^R,\tilde{\Gamma}_1^R,\Gamma_1^A,\tilde{\gamma}_1^A,x_1^K,\tilde{X}_1^K],\quad (28)$$

$$\check{g}_{2,\mathrm{in}}=\check{g}[\gamma_2^R,\tilde{\Gamma}_2^R,\Gamma_2^A,\tilde{\gamma}_2^A,x_2^K,\tilde{X}_2^K],\quad (29)$$

and the outgoing ones (with velocity direction away from the interface)

$$\check{g}_{1,\mathrm{out}}=\check{g}[\Gamma_1^R,\tilde{\gamma}_1^R,\gamma_1^A,\tilde{\Gamma}_1^A,X_1^K,\tilde{x}_1^K],\quad (30)$$

$$\check{g}_{2,\mathrm{out}}=\check{g}[\Gamma_2^R,\tilde{\gamma}_2^R,\gamma_2^A,\tilde{\Gamma}_2^A,X_2^K,\tilde{x}_2^K].\quad (31)$$

Using our parametrization, Zaitsev's boundary conditions can be solved for the unknown quantities in a straightforward way. In the superconducting state we define effective reflection and transmission coefficients, which we present in Appendix D. The sum of each generalized reflection coefficient with its corresponding transmission coefficient is equal to one. Using these coefficients we can write the general boundary conditions for the six unknown spin matrix distributions functions in a compact form. For the coherence functions we have[37]

$$\Gamma_1^{R,A}=R_{1l}^{R,A}\otimes\gamma_1^{R,A}+D_{1l}^{R,A}\otimes\gamma_2^{R,A}$$
$$=\gamma_1^{R,A}\otimes R_{1r}^{R,A}+\gamma_2^{R,A}\otimes D_{1r}^{R,A},\quad (32)$$

$$\tilde{\Gamma}_1^{R,A}=\tilde{R}_{1l}^{R,A}\otimes\tilde{\gamma}_1^{R,A}+\tilde{D}_{1l}^{R,A}\otimes\tilde{\gamma}_2^{R,A}$$
$$=\tilde{\gamma}_1^{R,A}\otimes\tilde{R}_{1r}^{R,A}+\tilde{\gamma}_2^{R,A}\otimes\tilde{D}_{1r}^{R,A}.\quad (33)$$

Note the intuitively appealing structure of the relations. The outgoing functions are weighted averages of two incoming functions. The weights depend on the incoming parameters as well, which reflects the coherence during Andreev reflection. The distribution functions have the following boundary conditions:

$$X_1^K=\frac{R_{1l}^R}{\mathcal{R}}\otimes\mathcal{R}x_1^K\otimes\frac{\tilde{R}_{1r}^A}{\mathcal{R}}+\frac{D_{1l}^R}{\mathcal{D}}\otimes\mathcal{D}x_2^K\otimes\frac{\tilde{D}_{1r}^A}{\mathcal{D}}$$
$$-A_{1l}^R\otimes\mathcal{R}D\tilde{x}_2^K\otimes\tilde{A}_{1r}^A,\quad (34)$$

$$\tilde{X}_1^K=\frac{\tilde{R}_{1l}^R}{\mathcal{R}}\otimes\mathcal{R}\tilde{x}_1^K\otimes\frac{R_{1r}^A}{\mathcal{R}}+\frac{\tilde{D}_{1l}^R}{\mathcal{D}}\otimes\mathcal{D}\tilde{x}_2^K\otimes\frac{D_{1r}^A}{\mathcal{D}}$$
$$-\tilde{A}_{1l}^R\otimes\mathcal{R}Dx_2^K\otimes A_{1r}^A.\quad (35)$$

Analogous relations, obtained by interchanging the subscripts 1 and 2, hold for the other side of the interface. The terms proportional to the product $\mathcal{R}D=\mathcal{D}(1-\mathcal{D})$, are due to particle-hole interference and do not arise in the classical limit. Insertion of these equations into Zaitsev's boundary conditions shows, that they solve the nonlinear problem and eliminate all spurious solutions.

VI. LINEAR RESPONSE THEORY

The general linear response theory in terms of the coherence functions and distribution functions was developed in Refs. 26 and 38. Here we give a short review of the relevant equations and generalize them for spin dependent phenomena. For the special case of the diamagnetic response see Belzig, Bruder, and Fauchère.[30] We assume a small external perturbation and expand $\check{g}$ and $\check{h}$ around the unperturbed solutions. With the replacements $\check{g}\to\check{g}+\delta\check{g}$ and $\check{h}\to\check{h}+\delta\check{h}$ we arrive in linear order at the equations

$$[\check{\epsilon}-\check{h},\delta\check{g}]_\otimes+i\hbar\mathbf{v}_f\boldsymbol{\nabla}\delta\check{g}=[\delta\check{h},\check{g}]_\otimes,\quad (36)$$

$$\delta\check{g}\otimes\check{g}+\check{g}\otimes\delta\check{g}=\check{0}.\quad (37)$$

Here the linearized self-consistency equations determine $\delta\check{h}$. For a specially chosen parametrization given at the end of Appendixes B and C, the linear correction of the Green's function $\delta\check{g}$ can be written in terms of the linear corrections to the coherence functions $\delta\gamma^{R,A}$, $\delta\tilde{\gamma}^{R,A}$ and linear corrections to the distribution functions δx^K, $\delta\tilde{x}^K$.

It is convenient to transform from the Keldysh response $\delta\hat{g}^K$ to the *anomalous response* $\delta\hat{g}^a$

$$\delta\hat{g}^a=\delta\hat{g}^K-\delta\hat{g}^R\otimes F_{\mathrm{eq}}+F_{\mathrm{eq}}\otimes\delta\hat{g}^A,\quad (38)$$

with $F_{\mathrm{eq}}=\tanh\epsilon/2T$. Using the anomalous self-energies

$$\delta\hat{h}^a=\delta\hat{h}^K-\delta\hat{h}^R\otimes F_{\mathrm{eq}}+F_{\mathrm{eq}}\otimes\delta\hat{h}^A,\quad (39)$$

we define the following short-hand notation for the driving terms in the transport equations:

$$\delta\hat{h}^{R,A}=\begin{pmatrix}\delta\Sigma^{R,A} & \delta\Delta^{R,A}\\ \delta\tilde{\Delta}^{R,A} & \delta\tilde{\Sigma}^{R,A}\end{pmatrix},\quad \delta\hat{h}^{a}=\begin{pmatrix}\delta\Sigma^{a} & \delta\Delta^{a}\\ -\delta\tilde{\Delta}^{a} & -\delta\tilde{\Sigma}^{a}\end{pmatrix}. \tag{40}$$

Then, with the definition of the anomalous components of the distribution spin matrices

$$\delta x^{a}=\delta x^{K}+\gamma^{R}\otimes F_{\mathrm{eq}}\otimes\delta\tilde{\gamma}^{A}+\delta\gamma^{R}\otimes F_{\mathrm{eq}}\otimes\tilde{\gamma}^{A}, \tag{41}$$

$$\delta\tilde{x}^{a}=\delta\tilde{x}^{K}-\tilde{\gamma}^{R}\otimes F_{\mathrm{eq}}\otimes\delta\gamma^{A}-\delta\tilde{\gamma}^{R}\otimes F_{\mathrm{eq}}\otimes\gamma^{A}, \tag{42}$$

the *spectral response* $\delta\hat{g}^{R,A}$ and the anomalous response $\delta\hat{g}^{a}$ together with the transport equations for the spin matrices $\delta\gamma^{R,A}$, $\delta\tilde{\gamma}^{R,A}$, δx^{a}, and $\delta\tilde{x}^{a}$, are given by

$$\delta\hat{g}^{R,A}=\mp 2\pi i\ \ \hat{N}^{R,A}\otimes\begin{pmatrix}(\delta\gamma^{R,A}\otimes\tilde{\gamma}^{R,A}+\gamma^{R,A}\otimes\delta\tilde{\gamma}^{R,A}) & (\delta\gamma^{R,A}+\gamma^{R,A}\otimes\delta\tilde{\gamma}^{R,A}\otimes\gamma^{R,A})\\ -(\delta\tilde{\gamma}^{R,A}+\tilde{\gamma}^{R,A}\otimes\delta\gamma^{R,A}\otimes\tilde{\gamma}^{R,A}) & -(\delta\tilde{\gamma}^{R,A}\otimes\gamma^{R,A}+\tilde{\gamma}^{R,A}\otimes\delta\gamma^{R,A})\end{pmatrix}\otimes\hat{N}^{R,A}, \tag{43}$$

$$\delta\hat{g}^{a}=-2\pi i\ \ \hat{N}^{R}\otimes\begin{pmatrix}(\delta x^{a}-\gamma^{R}\otimes\delta\tilde{x}^{a}\otimes\tilde{\gamma}^{A}) & -(\gamma^{R}\otimes\delta\tilde{x}^{a}-\delta x^{a}\otimes\gamma^{A})\\ -(\tilde{\gamma}^{R}\otimes\delta x^{a}-\delta\tilde{x}^{a}\otimes\tilde{\gamma}^{A}) & (\delta\tilde{x}^{a}-\tilde{\gamma}^{R}\otimes\delta x^{a}\otimes\gamma^{A})\end{pmatrix}\otimes\hat{N}^{A}, \tag{44}$$

$$\begin{aligned}i\hbar\mathbf{v}_{f}\boldsymbol{\nabla}\,\delta\gamma^{R,A}+2\epsilon\delta\gamma^{R,A}-(\gamma^{R,A}\tilde{\Delta}^{R,A}+\Sigma^{R,A})\otimes\delta\gamma^{R,A}+\delta\gamma^{R,A}\otimes(-\tilde{\Delta}^{R,A}\gamma^{R,A}+\tilde{\Sigma}^{R,A})\\ =\gamma^{R,A}\otimes\delta\tilde{\Delta}^{R,A}\otimes\gamma^{R,A}+\delta\Sigma^{R,A}\otimes\gamma^{R,A}-\gamma^{R,A}\otimes\delta\tilde{\Sigma}^{R,A}-\delta\Delta^{R,A},\end{aligned} \tag{45}$$

$$\begin{aligned}i\hbar\mathbf{v}_{f}\boldsymbol{\nabla}\,\delta\tilde{\gamma}^{R,A}-2\epsilon\delta\tilde{\gamma}^{R,A}-(\tilde{\gamma}^{R,A}\Delta^{R,A}+\tilde{\Sigma}^{R,A})\otimes\delta\tilde{\gamma}^{R,A}+\delta\tilde{\gamma}^{R,A}\otimes(-\Delta^{R,A}\tilde{\gamma}^{R,A}+\Sigma^{R,A})\\ =\tilde{\gamma}^{R,A}\otimes\delta\Delta^{R,A}\otimes\tilde{\gamma}^{R,A}+\delta\tilde{\Sigma}^{R,A}\otimes\tilde{\gamma}^{R,A}-\tilde{\gamma}^{R,A}\otimes\delta\Sigma^{R,A}-\delta\tilde{\Delta}^{R,A},\end{aligned} \tag{46}$$

$$\begin{aligned}i\hbar\mathbf{v}_{f}\boldsymbol{\nabla}\,\delta x^{a}+i\hbar\,\partial_{t}\delta x^{a}+(-\gamma^{R}\tilde{\Delta}^{R}-\Sigma^{R})\otimes\delta x^{a}+\delta x^{a}\otimes(-\Delta^{A}\tilde{\gamma}^{A}+\Sigma^{A})\\ =-\gamma^{R}\otimes\delta\tilde{\Sigma}^{a}\otimes\tilde{\gamma}^{A}+\delta\Delta^{a}\otimes\tilde{\gamma}^{A}+\gamma^{R}\otimes\delta\tilde{\Delta}^{a}-\delta\Sigma^{a},\end{aligned} \tag{47}$$

$$\begin{aligned}i\hbar\mathbf{v}_{f}\boldsymbol{\nabla}\,\delta\tilde{x}^{a}-i\hbar\,\partial_{t}\delta\tilde{x}^{a}+(-\tilde{\gamma}^{R}\Delta^{R}-\tilde{\Sigma}^{R})\otimes\delta\tilde{x}^{a}+\delta\tilde{x}^{a}\otimes(-\tilde{\Delta}^{A}\gamma^{A}+\tilde{\Sigma}^{A})\\ =-\tilde{\gamma}^{R}\otimes\delta\Sigma^{a}\otimes\gamma^{A}+\delta\tilde{\Delta}^{a}\otimes\gamma^{A}+\tilde{\gamma}^{R}\otimes\delta\Delta^{a}-\delta\tilde{\Sigma}^{a}.\end{aligned} \tag{48}$$

One convenient feature of our parametrization is the fact, that the linear response transport equations (45)–(48) decouple for given self-energies. Furthermore, the transport equations for $\delta\gamma^{R}$, $\delta\tilde{\gamma}^{A}$, δx^{a} are stable in direction of $\mathbf{v}_{f}$, and the transport equations for $\delta\tilde{\gamma}^{R}$, $\delta\gamma^{A}$, $\delta\tilde{x}^{a}$ are stable in direction of $-\mathbf{v}_{f}$. This makes a numerical treatment much easier than solving the boundary value problem for the coupled transport equations (36), (37). The **R** points for the initial condition correspond to the final point or the initial point of the trajectory depending on the direction of stability of the transport equation.

Finally we present the boundary conditions for the coherence functions and for the distribution functions in linear response. With an analogous definition of the anomalous components of the outgoing distribution spin matrices

$$\delta X^{a}=\delta X^{K}+\Gamma^{R}\otimes F_{\mathrm{eq}}\otimes\delta\tilde{\Gamma}^{A}+\delta\Gamma^{R}\otimes F_{\mathrm{eq}}\otimes\tilde{\Gamma}^{A}, \tag{49}$$

$$\delta\tilde{X}^{a}=\delta\tilde{X}^{K}-\tilde{\Gamma}^{R}\otimes F_{\mathrm{eq}}\otimes\delta\Gamma^{A}-\delta\tilde{\Gamma}^{R}\otimes F_{\mathrm{eq}}\otimes\Gamma^{A}, \tag{50}$$

we obtain the boundary conditions for the corrections to the coherence functions and distribution functions

$$\begin{aligned}\delta\Gamma_{1}^{R}=&\frac{R_{1l}^{R}}{\mathcal{R}}\otimes\mathcal{R}\,\delta\gamma_{1}^{R}\otimes\frac{R_{1r}^{R}}{\mathcal{R}}+\frac{D_{1l}^{R}}{\mathcal{D}}\otimes\mathcal{D}\,\delta\gamma_{2}^{R}\otimes\frac{D_{1r}^{R}}{\mathcal{D}}\\ &+A_{1l}^{R}\otimes\mathcal{R}\mathcal{D}\,\delta\tilde{\gamma}_{2}^{R}\otimes A_{1r}^{R},\end{aligned} \tag{51}$$

$$\begin{aligned}\delta\tilde{\Gamma}_{1}^{R}=&\frac{\tilde{R}_{1l}^{R}}{\mathcal{R}}\otimes\mathcal{R}\,\delta\tilde{\gamma}_{1}^{R}\otimes\frac{\tilde{R}_{1r}^{R}}{\mathcal{R}}+\frac{\tilde{D}_{1l}^{R}}{\mathcal{D}}\otimes\mathcal{D}\,\delta\tilde{\gamma}_{2}^{R}\otimes\frac{\tilde{D}_{1r}^{R}}{\mathcal{D}}\\ &+\tilde{A}_{1l}^{R}\otimes\mathcal{R}\mathcal{D}\,\delta\gamma_{2}^{R}\otimes\tilde{A}_{1r}^{R},\end{aligned} \tag{52}$$

$$\begin{aligned}\delta X_{1}^{a}=&\frac{R_{1l}^{R}}{\mathcal{R}}\otimes\mathcal{R}\,\delta x_{1}^{a}\otimes\frac{\tilde{R}_{1r}^{A}}{\mathcal{R}}+\frac{D_{1l}^{R}}{\mathcal{D}}\otimes\mathcal{D}\,\delta x_{2}^{a}\otimes\frac{\tilde{D}_{1r}^{A}}{\mathcal{D}}\\ &-A_{1l}^{R}\otimes\mathcal{R}\mathcal{D}\,\delta\tilde{x}_{2}^{a}\otimes\tilde{A}_{1r}^{A},\end{aligned} \tag{53}$$

$$\delta\tilde{X}_1^a=\frac{\tilde{R}_{1l}^R}{\mathcal{R}}\otimes\mathcal{R}\delta\tilde{x}_1^a\otimes\frac{R_{1r}^A}{\mathcal{R}}+\frac{\tilde{D}_{1l}^R}{\mathcal{D}}\otimes\mathcal{D}\delta\tilde{x}_2^a\otimes\frac{D_{1r}^A}{\mathcal{D}}$$
$$-\tilde{A}_{1l}^R\otimes\mathcal{R}D\,\delta x_2^a\otimes A_{1r}^A. \tag{54}$$

VII. ANDREEV SPECTROSCOPY AT *N-S* INTERFACES FOR UNCONVENTIONAL SUPERCONDUCTORS

To illustrate the physical content of the new distribution functions we discuss in this section the Andreev reflection process at an interface between a normal metal (subscript 1) and a *d*-wave superconductor (subscript 2). This problem was studied by Blonder, Tinkham, and Klapwijk[21] for conventional *s*-wave superconductors, and was generalized to unconventional superconductors by Bruder.[22] We generalize these calculations to include finite impurity scattering and identify features which are sensitive to time reversal symmetry breaking states. In an Andreev reflection experiment a beam of normal quasiparticles with energies ϵ_b and momenta $\mathbf{p}_{f,b}$ is injected across the interface into the superconductor. Two types of reflections will occur. Part of the beam will be regularly reflected at the interface, which amounts to a reflection of the quasiparticle's velocity, momentum, and current, and part will be Andreev reflected. Andreev's retroreflection is caused by particle-hole conversion which reverses the velocity but conserves momentum and current to very good approximation. Because the current is affected quite differently by regular reflection and Andreev reflection, a measurement of the current-voltage characteristics provides direct information on the balance between these two reflection processes. Together with a thorough theoretical analysis such measurements inform about fundamental properties of the superconductor such as the symmetry of pairing,[39] the gap size and anisotropies, and interface resonance states.[40–45] For anisotropic superconductors both the current density in the reflected and the Andreev reflected beams will depend strongly on the direction of the incoming beam, in addition to their dependence on the energy of the incoming quasiparticles.

The following calculation of Andreev reflection includes anisotropic pairing, a finite mean free path in the superconductor, a finite transparency of the normal-metal–superconductor (*N-S*) interface, the layer of a strongly distorted order parameter near the interface, and the effects of the interface on the excitation spectrum, in particular the low-energy bound states. We consider a layered *d*-wave superconductor with cylindrical Fermi surface and isotropic Fermi velocity along the layers. The interface lies perpendicular to the layers and we assume, for simplicity, the same Fermi velocity in the normal and the superconducting parts of the *N-S* contact.

The coherence functions γ_1^R, $\tilde{\gamma}_1^A$ are determined by boundary conditions at infinity, Eqs. (C7), (C8), whereas $\tilde{\Gamma}_1^R$, Γ_1^A are determined by the interface boundary conditions, Eqs. (32), (33). For the spin singlet superconductor we write $\gamma^R=i\sigma_y\gamma$, $\tilde{\gamma}^R=i\sigma_y\tilde{\gamma}$, $\Gamma^R=i\sigma_y\Gamma$, and $\tilde{\Gamma}^R=i\sigma_y\tilde{\Gamma}$, where γ, $\tilde{\gamma}$, Γ, $\tilde{\Gamma}$ are scalar functions. On the normal side the incoming coherence functions γ_1, $\tilde{\gamma}_1$ are zero as a consequence of their zero initial values at infinity. Thus, the retarded part of the Green's function on the normal side, following from Eqs. (28), (30), and (11), has the form

$$\hat{g}_{1,\mathrm{in}}^R=-i\pi\begin{pmatrix}1 & 0\\ -2i\sigma_y\tilde{\Gamma}_1 & -1\end{pmatrix}, \tag{55}$$

$$\hat{g}_{1,\mathrm{out}}^R=-i\pi\begin{pmatrix}1 & 2i\sigma_y\Gamma_1\\ 0 & -1\end{pmatrix}. \tag{56}$$

The nonzero quantities Γ_1 and $\tilde{\Gamma}_1$, describe the proximity effect at the *N-S* interface. The solutions for Γ_1 and $\tilde{\Gamma}_1$ in the normal metal in equilibrium are

$$\Gamma_1(x,\epsilon)=\Gamma_1(\epsilon)e^{i(2\epsilon/\hbar v_f)x}e^{-x/v_f\tau_1}, \tag{57}$$

$$\tilde{\Gamma}_1(x,\epsilon)=\tilde{\Gamma}_1(\epsilon)e^{-i(2\epsilon/\hbar v_f)x}e^{x/v_f\tau_1}, \tag{58}$$

where the spatial trajectory coordinate x is measured in direction of $\mathbf{v}_f$ and is zero at the interface, positive for Γ_1 and negative for $\tilde{\Gamma}_1$, and τ_1 is the lifetime in the normal metal. Both amplitudes decay from the interface towards the normal metal on a scale $v_f\tau_1$. For simplicity, we assume in all what follows that the normal metal is in the clean limit. The Tomasch oscillation factors,[15] with Tomasch wave length $\pi\hbar v_f/\epsilon$, are carried by Γ_1, $\tilde{\Gamma}_1$, whereas γ_2^R and $\tilde{\gamma}_2^A$ vary only in the region of varying order parameter near the interface and are constant far away. Similarly, on the superconducting side, far away from the interface, the deviations of the outgoing coherence functions from their homogeneous solutions $\Gamma_2(x)-\Gamma_{2,\mathrm{hom}}$, $\tilde{\Gamma}_2(x)-\tilde{\Gamma}_{2,\mathrm{hom}}$, carry the Tomasch oscillations with wavelength $\pi\hbar v_f/\sqrt{\epsilon^2-|\Delta|^2}$ if $|\epsilon|>|\Delta|$. In the following all quantities without spatial argument refer to their values at the interface.

In quasiclassical approximation the incoming beam of nonequilibrium excitations with energy, ϵ_b, and momentum $\mathbf{p}_{f,b}$ is described by the ''scattering'' part of the Keldysh Green's function $\Delta\hat{g}^K=\hat{g}^K-\hat{g}_{\mathrm{eq}}^K$, where the equilibrium Keldysh Green's function $\hat{g}_{\mathrm{eq}}^K$ is subtracted. In the following we assume, for simplicity, a spin unpolarized incoming beam. The calculations for spin-polarized beams pose no new problems but are of interest only for high-field superconductivity,[46] spin-triplet pairing,[47–50] contacts between superconductors and magnetic materials,[51] or spin-active interfaces.[32,51] The incoming beam is then characterized by unit spin-matrix distribution functions Δx_1^K and $\Delta\tilde{X}_1^K$. To obtain a physical interpretation of this distribution functions we consider a solution of Eq. (16) in form of a traveling wave with frequency ω,

$$\Delta x_1^K(x,\epsilon,t)=\Delta x_1^K(\epsilon)e^{i(\omega/v_f)(x-v_ft)}. \tag{59}$$

The corresponding part of the Keldysh Green's function follows from Eq. (12), and after performing the time convolutions, Eq. (A1), we obtain

$$\Delta\hat{g}^K_{1,\mathrm{in}}(x,\epsilon,t) = -2\pi i \times \left\{ \Delta x^K_1(\epsilon) \begin{pmatrix} e^{i(\omega/v_f)(x-v_f t)} & -i\sigma_y \tilde{\Gamma}^*_1\left(\epsilon - \frac{\hbar\omega}{2}\right) e^{i(k_T x-\omega t)} \\ -i\sigma_y \tilde{\Gamma}_1\left(\epsilon + \frac{\hbar\omega}{2}\right) e^{-i(k_T x+\omega t)} & -\tilde{\Gamma}_1\left(\epsilon + \frac{\hbar\omega}{2}\right)\tilde{\Gamma}^*_1\left(\epsilon - \frac{\hbar\omega}{2}\right) e^{-i(\omega/v_f)(x+v_f t)} \end{pmatrix} + \begin{pmatrix} 0 & 0 \\ 0 & \Delta\tilde{X}^K_1(x,\epsilon,t) \end{pmatrix} \right\}, \tag{60}$$

where $k_T = 2\epsilon/\hbar v_f$ is the Tomasch wave vector. This gives us a very transparent interpretation for the processes covered by Δx^K_1. The upper left entry describes an incoming particle with velocity v_f. The lower right entry describes an Andreev reflected hole with velocity $-v_f$, coming from the interface due to retroreflection combined with particle hole conversion. The off-diagonal components describe particle- and holelike Tomasch oscillations due to particle-hole coherence. The degree of coherence between particles and holes in the incoming distribution Δx^K_1 is given by the coherence function $\tilde{\Gamma}_1$. This gives a direct physical interpretation of the coherence functions. Similarly, Γ_1 is the amplitude for Andreev reflected particles due to an incoming hole excitation beam. On the other hand, the distribution function $\Delta\tilde{X}^K_1$ describes an incoherent hole coming from the interface. This component can be nonzero only if there is an incoming hole in the Green's function $\Delta\hat{g}^K_{1,\mathrm{out}}$ or $\Delta\hat{g}^K_{2,\mathrm{out}}$, which we exclude in our scattering boundary condition. Thus, the correct boundary conditions for the scattering problem take the intuitively appealing form, to allow for the incoming particle beam only an incoming distribution function Δx^K_1 and for all outgoing channels only outgoing distribution functions ΔX^K_1, ΔX^K_2, $\Delta\tilde{X}^K_2$. All other distribution function components are zero.

In the following we assume a stationary ($\omega = 0$) situation, where an incoherent beam is injected, which allows us to consider the incoming beam spatially homogeneous along the trajectory. Furthermore, it is sufficient to solve the problem for the distribution function

$$\Delta x^K_1 = -8\pi\delta\epsilon\,\delta(\epsilon-\epsilon_b)\,\delta(\hat{\mathbf{p}}_f - \hat{\mathbf{p}}_{f,b}), \tag{61}$$

where $\hat{\mathbf{p}}_f$ denotes a unit vector in direction $\mathbf{p}_f$, and $\delta\epsilon$ is the energy resolution of the beam. Any other distribution of incoming excitations is then given by a linear combination of such solutions with properly chosen weight functions. The current density of the incoming beam is $j_0 = 2eN_f v_f \delta\epsilon$. For a current density much smaller than the critical current density in the superconductor, one can neglect the effect of the beam on the self-consistent order parameter and impurity self-energies.

For the scattering parts of the Keldysh Green's function at the normal side we obtain

$$\Delta\hat{g}^K_{1,\mathrm{in}} = -2\pi i \Delta x^K_1 \begin{pmatrix} 1 & -i\sigma_y\tilde{\Gamma}^*_1 \\ -i\sigma_y\tilde{\Gamma}_1 & -|\tilde{\Gamma}_1|^2 \end{pmatrix}, \tag{62}$$

$$\Delta\hat{g}^K_{1,\mathrm{out}} = -2\pi i \Delta X^K_1 \begin{pmatrix} 1 & 0 \\ 0 & 0 \end{pmatrix}. \tag{63}$$

The vanishing off-diagonal elements of the reflected Green's function show that there is no hole admixing in the reflected particle beam.

The boundary conditions for the *N*-*S* interface follow from Eqs. (32)–(35),

$$\Delta X^K_1 = \mathcal{R}\left|\frac{1+\gamma_2\tilde{\gamma}_2}{1+\mathcal{R}\gamma_2\tilde{\gamma}_2}\right|^2 \Delta x^K_1, \tag{64}$$

$$\Delta X^K_2 = \mathcal{D}\Delta x^K_1, \quad \Delta\tilde{X}^K_2 = -\mathcal{R}D|\tilde{\gamma}_2|^2\Delta x^K_1, \tag{65}$$

$$\Gamma_1 = \mathcal{D}\frac{\gamma_2}{1+\mathcal{R}\gamma_2\tilde{\gamma}_2}, \quad \Gamma_2 = \mathcal{R}\gamma_2, \tag{66}$$

$$\tilde{\Gamma}_1 = \mathcal{D}\frac{\tilde{\gamma}_2}{1+\mathcal{R}\gamma_2\tilde{\gamma}_2}, \quad \tilde{\Gamma}_2 = \mathcal{R}\tilde{\gamma}_2. \tag{67}$$

The total current densities are given in terms of the Keldysh Green's functions via the formula $\mathbf{j} = eN_f\int(d\epsilon/8\pi i)\mathrm{Tr}\langle\tau_3\mathbf{v}_f\Delta\hat{g}^K\rangle$.[4] Using the boundary conditions (64)–(67), this gives directly the total current densities at the interface in terms of the injected current density

$$\frac{j_{1,\mathrm{in}}}{j_0} = 1+\mathcal{D}^2\left|\frac{\tilde{\gamma}_2}{1+\mathcal{R}\tilde{\gamma}_2\gamma_2}\right|^2, \tag{68}$$

$$\frac{j_{1,\mathrm{out}}}{j_0} = \mathcal{R}\left|\frac{1+\gamma_2\tilde{\gamma}_2}{1+\mathcal{R}\gamma_2\tilde{\gamma}_2}\right|^2, \tag{69}$$

$$\frac{j_{2,\mathrm{in}}}{j_0} = \mathcal{R}\mathcal{D}\frac{|\tilde{\gamma}_2|^2(1+|\gamma_2|^2)}{|1+\mathcal{R}\tilde{\gamma}_2\gamma_2|^2}, \tag{70}$$

$$\frac{j_{2,\mathrm{out}}}{j_0} = \mathcal{D}\frac{1+|\tilde{\gamma}_2|^2}{|1+\mathcal{R}\gamma_2\tilde{\gamma}_2|^2}. \tag{71}$$

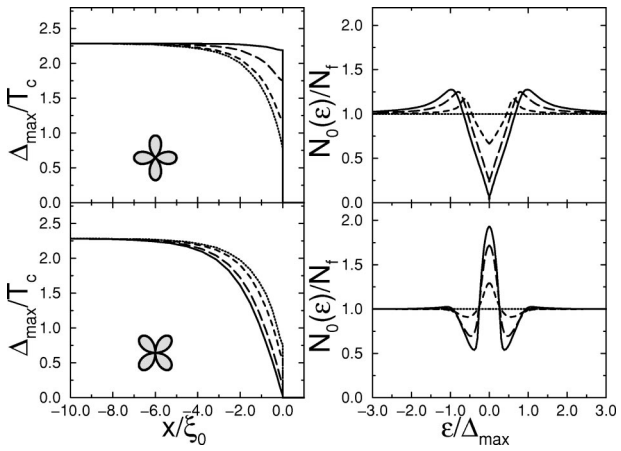

FIG. 2. Order parameter amplitude (left) and local density of states at the interface (right) for an interface between a *d*-wave superconductor and a normal metal, in (100) direction (top) and in (110) direction (bottom). The interface is at $x=0$, the normal metal extends to $x>0$. The transmission coefficients for the different curves are $\mathcal{D}_0=0.1$ (full line), $\mathcal{D}_0=0.5$ (long dashed), $\mathcal{D}_0=0.9$ (dashed), and $\mathcal{D}_0=1.0$ (dotted). The temperature is $T=0.3T_c$, and the mean free path $l=10\xi_0$.

Here, $j_{1,\mathrm{in}}$ describes the incoming current including the excess current, $j_{2,\mathrm{in}}$ the regularly reflected current, $j_{2,\mathrm{out}}$ the regularly transmitted current, and $j_{2,\mathrm{in}}$ describes the process where the Andreev reflected holes are regularly reflected back to the superconductor at the interface. For energies below the gap the transmitted current densities $j_{2,\mathrm{in}}$, $j_{2,\mathrm{out}}$, decay with distance from the interface into the superconducting region, where they are converted into super-currents. It is straightforward to show the conservation law $j_{1,\mathrm{in}}+j_{2,\mathrm{in}}=j_{1,\mathrm{out}}+j_{2,\mathrm{out}}$. Eqs. (68)–(71) hold for general anisotropic and unconventional superconductors, including impurity scattering. The quantities γ_2 and $\tilde{\gamma}_2$ follow from solving numerically their transport equations, Eqs. (14) and (15), with self-consistently determined self-energies and order parameter. For conventional *s*-wave superconductors, and assuming a step function for the order parameter our formulas agree with the results of Blonder, Tinkham, and Klapwijk.[21] It is clear from Eq. (68) that the Andreev reflected beam always enhances the current density in the injection beam, giving rise to the excess current. The enhancement is proportional to $\mathcal{D}^2$, reflecting the fact that both the incoming particle and the Andreev reflected hole have to cross the interface. On the other hand, the current density of the conventionally reflected beam, described by Eq. (69), can be below or above the value $\mathcal{R}\cdot j_0$.

The angle resolved density of states at the superconducting side of the interface is given by

$$N(\epsilon,\mathbf{p}_f)=N_f\mathrm{Re}\frac{1-\mathcal{R}\gamma_2\tilde{\gamma}_2}{1+\mathcal{R}\gamma_2\tilde{\gamma}_2}. \tag{72}$$

The local density of states is given by the Fermi surface average over this expression. Equation (72) shows that interface bound states are given by the solution of the equation $1+\mathcal{R}\gamma_2\tilde{\gamma}_2=0$. Because the absolute values of γ_2 and $\tilde{\gamma}_2$ are in equilibrium always smaller than or equal to unity, bound states at an interface can strictly occur only for $\mathcal{R}=1$, that means zero transmission. For finite transmission the bound states broaden into interface resonances. Impurity scattering further broadens these resonances. In Fig. 2 we show our self-consistent solutions for the *d*-wave order parameter $\Delta=\sqrt{2}\cos 2\psi$ and for the local density of quasiparticle states at the interface. For definiteness, we modeled the angular dependence of the transmission coefficient for the *N*-*N* interface by

$$\mathcal{D}(\phi)=\frac{\mathcal{D}_0\sin^2\phi}{\mathcal{R}_0+\mathcal{D}_0\sin^2\phi}, \tag{73}$$

appropriate for a δ-function potential barrier. Here, ϕ is the impact angle between incoming trajectory and interface. The parameters $\mathcal{D}_0$ and $\mathcal{R}_0=1-\mathcal{D}_0$ are the transmission and reflection coefficients for perpendicular impact ($\phi=\pi/2$). The impurity self-energy was calculated self-consistently in Born approximation with a mean free path of $l=10\xi_0$. The temperature was chosen $T=0.3T_c$, leading to a maximal gap of $\Delta_{\max}=2.29T_c$. For the (100) orientation of the interface the order parameter is constant in the superconductor for zero transmission and is suppressed at the interface for finite transmission. In contrast for the (110) orientation the order parameter is suppressed to zero at the surface for $\mathcal{D}=0$ and is suppressed to a finite value if $\mathcal{D}$ is nonzero.[22] In the (100) orientation there is no subgap resonance, whereas a zero energy resonance typical for *d*-wave pairing at properly oriented surfaces is present at (110) orientation.[41] Above the maximal gap the density of states is enhanced for (100) orientation. There is no such enhancement in the density of states at the interface above the gap for (110) orientation.

Figures 3 and 4 show selected results of our calculations of Andreev reflection at a contact between a normal metal and a *d*-wave superconductor. Our calculations are done for $T=0.3T_c$, for three mean free paths $l=2\xi_0, 10\xi_0$, $100\xi_0$, and for two orientations of the interface. Figure 3 shows for three energies the dependence of the excess current due to Andreev reflection (top panels) and the regularly reflected current (bottom panels) on the impact angle for transmissions $\mathcal{D}_0=0.5$ (left picture) and for transmission $\mathcal{D}_0=0.9$ (right picture). The positions of the gap nodes show up clearly in the Andreev reflection amplitude, which breaks down for quasiparticles transmitted into the nodal directions. The regular reflection approaches for the nodal direction the value $\mathcal{R}(\phi)$. The width of this breakdown regions broadens with energy. At energies above the maximal gap $\Delta_{\max}$, the Andreev amplitude approaches zero and the regularly reflected amplitude approaches the value $\mathcal{R}(\phi)$. The dependence on the energy of the incoming quasiparticles is shown for one representative impact angle in Fig. 4 for three values of mean free path, again for transmission $\mathcal{D}_0=0.5$ (left) and for transmission $\mathcal{D}_0=0.9$ (right). For the (100) interface as shown in Figs. 3 and 4, the behavior at low energies is clearly distinct from the behavior for a (110) interface. Whereas for a (110) interface the regular reflection is suppressed for low energies, it is enhanced for a (100) interface. The excess current shows a peak at low energies for the (110) interface, but the (100) interface shows a minimum. The features at the gap edges are small for the (110) orientation, but are strong for the (100) orientation. And finally,

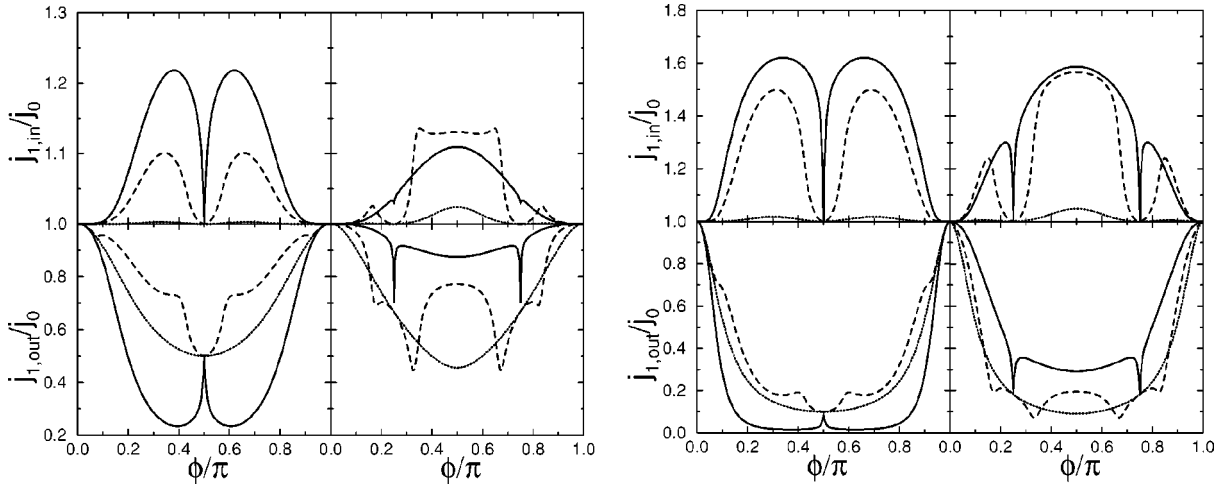

FIG. 3. Current densities in the injected beam (top panels) and in the regularly reflected beam (bottom panels), as a function of the impact angle for three energies: $\epsilon_b=0$ (full line), $0.4\Delta_{\max}$ (dashed), and $1.6\Delta_{\max}$ (dotted). The left part of each picture is for a (110) interface, and the right part of each picture for a (100) interface between a *d*-wave superconductor and a normal metal. The left picture is for a transmission coefficient $\mathcal{D}_0=0.5$, and the right picture for a transmission coefficient $\mathcal{D}_0=0.9$. The temperature is $T=0.3T_c$, and the mean free path $l=10\xi_0$.

the signal above the gap edges is small for a (110) interface but extends well up to twice the gap for a (100) interface.

In the clean limit the zero energy current density of the incoming beam is $j_{1,\mathrm{in}}/j_0=2$ for a (110) interface, and $j_{1,\mathrm{in}}/j_0=2(1+\mathcal{R}^2)/(1+\mathcal{R})^2\leqslant 2$ for a (100) interface; for the regularly reflected beam the zero energy limit is $j_{1,\mathrm{out}}/j_0=0$ for a (110) interface, and $j_{1,\mathrm{out}}/j_0=4\mathcal{R}/(1+\mathcal{R})^2\geqslant\mathcal{R}$ for a (100) interface. The values for the (100) interface coincide with the values for a conventional isotropic *s*-wave superconductor, and are in agreement with Blonder *et al.*[21] and Shelankov.[52] Explicit values for the zero energy limits at a (100) surface are for perpendicular impact $j_{1,\mathrm{in}}/j_0=1.11$, $j_{1,\mathrm{out}}/j_0=0.89$ for $\mathcal{D}=0.5$, and $j_{1,\mathrm{in}}/j_0=1.67$, $j_{1,\mathrm{out}}/j_0=0.33$ for $\mathcal{D}=0.9$. These values agree with our numerical calculations for mean free paths $l\geqslant 100\xi_0$. In contrast, the zero energy values for the (110) interface of two for the incoming and of zero for the reflected beam are very sensitive to impurity scattering. In fact, as can be seen from Fig. 4, is the first value reduced to about 1.2 for half transmission and a realistic mean free path of ten coherence lengths, and the second value is larger than 0.2 in this case. Also the structures around the gap edges for the (100) surface are very sensitive to impurity scattering. For a mean free path of two coherence lengths the Andreev signal is already strongly reduced, as our calculations in Fig. 4 show. This may explain the small signal of only a few percent in many Andreev experiments. The different behavior at low energies for the *regular* reflection is the only remaining difference between (100) and (110) orientation for mean free paths comparable to the coherence length for unconventional su-

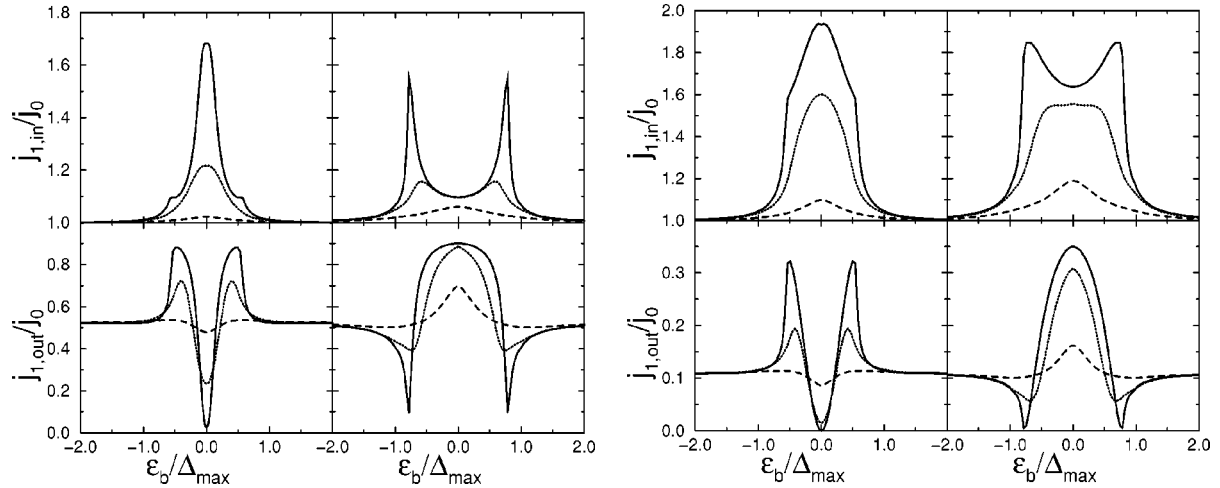

FIG. 4. Current densities in the injected beam (top panels) and in the regularly reflected beam (bottom panels), as a function of energy for three different mean free path values for the superconductor: $l=100\xi_0$ (full line), $10\xi_0$ (dotted), and $2\xi_0$ (dashed). The impact angle is $\phi/\pi=0.4$. The left part of each picture is for a (110) interface, and the right part of each picture for a (100) interface between a *d*-wave superconductor and a normal metal. The left picture is for a transmission coefficient $\mathcal{D}_0=0.5$, and the right picture for a transmission coefficient $\mathcal{D}_0=0.9$. The temperature is $T=0.3T_c$. The values for the maximal gaps at this temperature are $\Delta_{\max}(l=100\xi_0)=2.13T_c(l=100\xi_0)$, $\Delta_{\max}(l=10\xi_0)=2.29T_c(l=10\xi_0)$, $\Delta_{\max}(l=2\xi_0)=2.85T_c(l=2\xi_0)$.

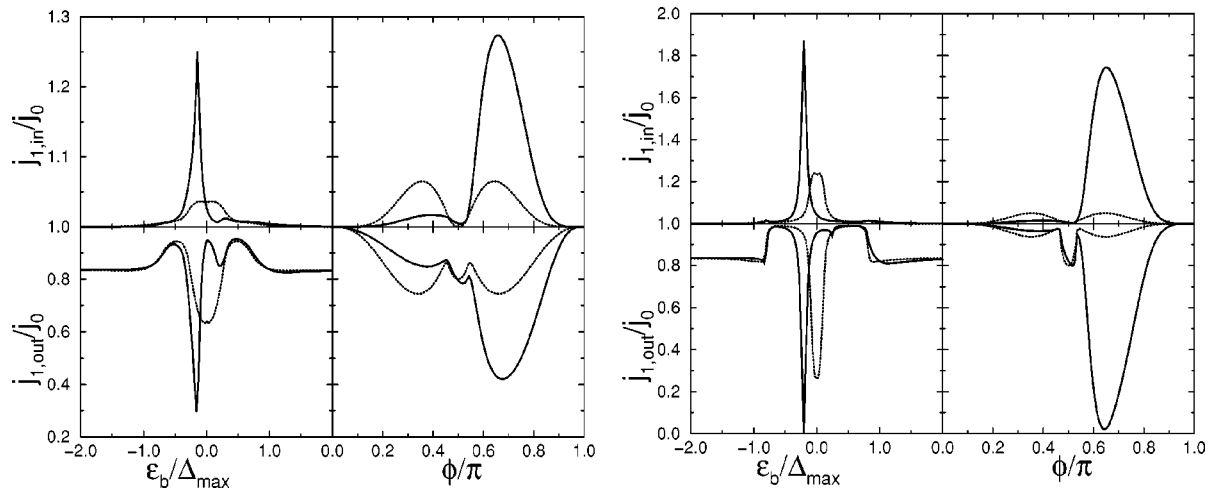

FIG. 5. Current densities in the injected beam (top panels) and in the regularly reflected beam (bottom panels) at a (110) interface. Dotted lines are for a temperature $T=0.3T_d$, which is above the transition temperature from a d to a $d+is$ state. Full lines are for a temperature $T=0.1T_d$, which is below this transition to the spontaneaously time reversal symmetry broken state. The left picture is for mean free path $l=10\xi_0$, and the right picture for mean free path $l=100\xi_0$. The left part in each picture shows the energy dependence for impact angle $\phi/\pi=0.348$, and the right part of each picture shows the dependence on impact angle for $\epsilon=0.2\Delta_{\max}$. The transmission coefficient is $\mathcal{D}_0=0.2$. The subdominant transition temperature is $T_{s,0}=0.3T_c$.

perconductors. The suppression of the regularly reflected beam at low energies for all angles (except in nodal direction), as seen for a (110) interface in the lower left panels of Figs. 3 and 4, is a direct consequence of the sign change of the order parameter during reflection of quasiparticles. The origin of this effect is the same as for the zero energy resonance (and follows from the Atiyah-Patodi-Singer theorem[53]). Both effects are destroyed by time reversal symmetry breaking and both effects are washed out by impurity scattering. However, in contrast to the zero energy resonance, which is not an exact bound state anymore for finite transmission even for zero impurity scattering, the strong suppression at low energies of the regularly reflected beam remains a stable phenomenon for all transmissions in the clean limit. The effect is reduced by finite impurity scattering, and in this case it is further reduced if the transmission is comparable or smaller than the scattering rate. Thus, the zero-energy resonance and the blocking of the regular reflection are two complementary phenomena: the first one is well established only for interfaces with small transmissions, whereas the latter one is well established at interfaces where the transmission is not too small.

The low-energy behavior of the regularly reflected beam can be used to prove a sign change of the order parameter during reflection of the quasiparticles at an interface. Specifically, our results show that at low energies for all impact angles this reflection amplitude is always *above* the normal state reflection, $\mathcal{R}(\phi)$, whereas for the (110) interface it is for all directions clearly *below* $\mathcal{R}(\phi)$ (the normal state reflection can be obtained for a beam with ϵ_b well above the maximal gap).

Finally, we show that the low-energy suppression of the regular reflection and enhancement of the excess current is a sensitive test for time reversal symmetry breaking states. In Fig. 5 we show our results for a dominant d-wave coupled to a subdominant s-wave component. Below the interface transition[42,54,55] they couple to the spontaneously time reversal symmetry breaking state $d+is$,[42,54] where the s-wave component is localized in a layer of a few coherence lengths near the interface. The left picture is for $l=10\xi_0$ and the right picture for $l=100\xi_0$ The coupling strength of the subdominant component is characterized by its ''bare'' transition temperature $T_{s,0}$ (in the absence of the dominant component). This transition temperature is reduced in the presence of the dominant component.[42,54,55] We chose $T_{s,0}=0.3T_d$, where T_d is the transition temperature from the normal state to the pure d-wave state. This value of $T_{s,0}$ is below the critical value for a possible transition into a bulk $d+is$ state.[42] Nevertheless, the transition into a $d+is$ state localized near the interface is possible. According to our calculations the subdominant component is strongly suppressed by finite transmission, so we chose a small value $\mathcal{D}_0=0.2$. The dotted curves show the current densities of the reflected beams for a temperature $T=0.3T_d$. The system is at this temperature above the transition into the time reversal symmetry breaking state. Full curves are for $T=0.1T_d$, which corresponds to the interface $d+is$ state. As can be seen from Fig. 5, the suppression of the reflection and the enhancement of Andreev reflection are shifted to negative energies. Due to finite impurity scattering, and resulting mixing of different momentum directions, there is also a shadow-feature at positive energies. The broadening of the feature itself is reduced, leading to a much sharper effect compared to the pure d-wave state. The zero energy values for regular reflection are changed in the $d+is$ state to almost 1. Also shown in Fig. 5 is the dependence of the reflected current densities on the impact angle. The small dip at $\phi=\pi/2$ is due to the fact that the energy of the incoming particles is above the gap in these directions. Below the transition into the $d+is$ state there is a strong anisotropy with respect to the interface normal. This effect is a consequence of the spontaneous supercurrents at the superconducting side of the interface.[56] For an incoming particle beam with a projection on the interface counter-moving with the current the regular reflection is strongly reduced compared to the pure d-wave state, whereas

the Andreev reflection is enhanced for this case. For a beam with a projection comoving with the supercurrent these effects are absent or inverted. The shift of the feature in the energy dependence of the reflected current densities is determined by the Doppler shift of the quasiparticle spectrum due to the spontaneous supercurrent at the superconducting side of the interface. Thus, the *sign* of the shift for a chosen impact angle can be positive or negative dependent on the direction of the spontaneous interface currents (similarly the asymmetry around the interface normal changes its sign).

VIII. CONCLUSIONS

We have developed a theoretical formulation of nonequilibrium superconducting phenomena, including singlet and triplet pairing, in terms of coherence functions and distribution functions. Our central results are Eqs. (11)–(17), together with boundary conditions at interfaces, Eqs. (32)–(35). We used this formulation to present the theory for Andreev spectroscopy at interfaces between a normal metal and an unconventional superconductor in a transparent way. This formulation allows to include disorder in a self-consistent manner. We proposed an anomalous suppression of the regularly reflected quasiparticle beam as a test for time reversal symmetry breaking states. This test is especially suitable for not too small transmission, where the zero energy interface resonances become ill-defined and cannot be used as a test for time-reversal symmetry breaking anymore.

ACKNOWLEDGMENTS

I gratefully acknowledge useful discussions with L. Buchholtz, M. Fogelström, J. Moreno, D. Rainer, J. A. Sauls, and S.-K. Yip. This work was supported by the National Science Foundation (DMR 91-20000) through the Science and Technology Center for Superconductivity, and by the Deutsche Forschungsgemeinschaft. Part of the work was performed at the Aspen Center of Physics.

APPENDIX A: NOTATION

The noncommutative $\otimes$ product is defined in the following way:

$$\hat{A}\otimes\hat{B}(\epsilon,t)=e^{(i\hbar/2)(\partial_\epsilon^A\partial_t^B-\partial_t^A\partial_\epsilon^B)}\hat{A}(\epsilon,t)\hat{B}(\epsilon,t). \tag{A1}$$

If one of the factors is both independent of ϵ and t, the $\otimes$ product reduces to the usual matrix product.

For Fourier transformed quantities ($t\to\omega$) we have

$$\hat{A}\otimes\hat{B}(\epsilon,\omega)=\int_{-\infty}^{\infty}\frac{d\omega'}{2\pi}\frac{d\omega''}{2\pi}\delta(\omega'+\omega''-\omega)\times\hat{A}\left(\epsilon+\frac{\hbar\omega'}{2},\omega''\right)\hat{B}\left(\epsilon-\frac{\hbar\omega''}{2},\omega'\right). \tag{A2}$$

If $\hat{A}(\epsilon,t)=\hat{A}(\epsilon)$ is independent of t, that means, $\hat{A}$ is an equilibrium quantity, then

$$\hat{A}\otimes\hat{B}(\epsilon,\omega)=\hat{A}\left(\epsilon+\frac{\hbar\omega}{2}\right)\hat{B}(\epsilon,\omega), \tag{A3}$$

and, analogously, if $\hat{B}$ is an equilibrium quantity

$$\hat{A}\otimes\hat{B}(\epsilon,\omega)=\hat{A}(\epsilon,\omega)\hat{B}\left(\epsilon-\frac{\hbar\omega}{2}\right). \tag{A4}$$

Also we generalize the commutator

$$[\hat{A},\hat{B}]_\otimes=\hat{A}\otimes\hat{B}-\hat{B}\otimes\hat{A}. \tag{A5}$$

The Fermi surface average $\langle\cdots\rangle_{\mathbf{p}'}$ is defined by

$$\langle\cdots\rangle_{\mathbf{p}_f'}=\frac{1}{N_f}\int\frac{d^2\mathbf{p}_f'}{(2\pi\hbar)^3|\mathbf{v}_f(\mathbf{p}_f')|}\cdots, \tag{A6}$$

where N_f is the total density of states at the Fermi surface in the normal state

$$N_f=\int\frac{d^2\mathbf{p}_f'}{(2\pi\hbar)^3|\mathbf{v}_f(\mathbf{p}_f')|} \tag{A7}$$

and $\mathbf{v}_f(\mathbf{p}_f')$ is the normal state Fermi velocity at the position $\mathbf{p}_f'$ on the Fermi surface

$$\mathbf{v}_f(\mathbf{p}_f')=\frac{\partial\varepsilon(\mathbf{p})}{\partial\mathbf{p}}\Big|_{\mathbf{p}=\mathbf{p}_f'}. \tag{A8}$$

Here, $\varepsilon(\mathbf{p})$ describes the normal state dispersion of the quasiparticle band crossing the Fermi level at $\mathbf{p}_f'$.

APPENDIX B: PROJECTORS

Following Shelankov,[18] we introduce the following projectors:

$$\check{P}_\pm=\frac{1}{2}\left(\check{1}\pm\frac{1}{-i\pi}\check{g}\right). \tag{B1}$$

From the normalization condition, $\check{g}\otimes\check{g}=-\pi^2\check{1}$, it follows that $\check{P}_+$ and $\check{P}_-$ are projection operators

$$\check{P}_+\otimes\check{P}_+=\check{P}_+,\quad \check{P}_-\otimes\check{P}_-=\check{P}_- \tag{B2}$$

and project orthogonal to each other

$$\check{P}_++\check{P}_-=\check{1}, \tag{B3}$$

$$\check{P}_+\otimes\check{P}_-=\check{P}_-\otimes\check{P}_+=\check{0}. \tag{B4}$$

The quasiclassical Green's functions may be expressed in terms of $\check{P}_+$ or $\check{P}_-$,

$$\check{g}=-i\pi(\check{P}_+-\check{P}_-)$$
$$=-i\pi(2\check{P}_+-\check{1})=-i\pi(\check{1}-2\check{P}_-). \tag{B5}$$

Equations of motion for the projectors can be extracted from the corresponding equations for the quasiclassical Green's functions

$$[\check{\epsilon}-\check{h},\check{P}_\pm]_\otimes+i\hbar\mathbf{v}_f\nabla\check{P}_\pm=\check{0}. \tag{B6}$$

The Keldysh component of the Green's functions $\hat{g}^K$ fulfills the relation $\hat{g}^R\otimes\hat{g}^K+\hat{g}^K\otimes\hat{g}^A=\hat{0}$. This implies $\hat{P}_+^R\otimes\hat{g}^K\otimes\hat{P}_+^A=\hat{0}$ and $\hat{P}_-^R\otimes\hat{g}^K\otimes\hat{P}_-^A=\hat{0}$, leading to

$$\hat{g}^K=\hat{P}_+^R\otimes\hat{g}^K\otimes\hat{P}_-^A+\hat{P}_-^R\otimes\hat{g}^K\otimes\hat{P}_+^A. \tag{B7}$$

The value of $\hat{P}_+^R\otimes\hat{g}^K\otimes\hat{P}_-^A$ does not determine $\hat{g}^K$ uniquely. It is possible to add $\hat{P}_-^R\otimes\hat{A}+\hat{B}\otimes\hat{P}_+^A$ to $\hat{g}^K$ with any matrix function $\hat{A}$ and $\hat{B}$ without changing $\hat{P}_+^R\otimes\hat{g}^K\otimes\hat{P}_-^A$ (similarly

for $\hat{P}^R_- \otimes \hat{g}^K \otimes \hat{P}^A_+$). One can use this property to obtain a proper parametrization of $\hat{g}^K$ and to eliminate the unnecessary information in $\hat{g}^K$. We write

$$\hat{g}^K = -2\pi i(\hat{P}^R_+ \otimes \hat{X}^K \otimes \hat{P}^A_- + \hat{P}^R_- \otimes \hat{Y}^K \otimes \hat{P}^A_+), \quad \text{(B8)}$$

where $\hat{X}^K$ and $\hat{Y}^K$ contain only one free spin matrix function as parameter. The $\hat{X}^K$ and $\hat{Y}^K$ have to fulfill fundamental symmetry relations, following from the symmetry relations for the quasiclassical Green's function, $\breve{g}$. From the equations of motion of the Keldysh Green's functions

$$(\epsilon\hat{\tau}_3 - \hat{h}^R)\otimes\hat{g}^K - \hat{g}^K\otimes(\epsilon\hat{\tau}_3 - \hat{h}^A) + i\hbar\mathbf{v}_f\boldsymbol{\nabla}\hat{g}^K = -(\hat{g}^R\otimes\hat{h}^K - \hat{h}^K\otimes\hat{g}^A), \quad \text{(B9)}$$

we obtain the equations of motion for $\hat{X}^K$ and $\hat{Y}^K$ using Eq. (B6)

$$\hat{P}^R_+\otimes\{(\epsilon\hat{\tau}_3 - \hat{h}^R)\otimes\hat{X}^K - \hat{X}^K\otimes(\epsilon\hat{\tau}_3 - \hat{h}^A) + \hat{h}^K + i\hbar\mathbf{v}_f\boldsymbol{\nabla}\hat{X}^K\}\otimes\hat{P}^A_- = \hat{0}, \quad \text{(B10)}$$

$$\hat{P}^R_-\otimes\{(\epsilon\hat{\tau}_3 - \hat{h}^R)\otimes\hat{Y}^K - \hat{Y}^K\otimes(\epsilon\hat{\tau}_3 - \hat{h}^A) - \hat{h}^K + i\hbar\mathbf{v}_f\boldsymbol{\nabla}\hat{Y}^K\}\otimes\hat{P}^A_+ = \hat{0}. \quad \text{(B11)}$$

Tracing these equations properly in the Nambu space and respecting the symmetries of $\hat{X}^K$ and $\hat{Y}^K$, one obtains two equations for both undetermined 2×2 spin matrix functions, which parametrize $\hat{X}^K$ and $\hat{Y}^K$.

Analogously we proceed for the linear response. From the first-order normalization conditions (37) we have $\hat{P}^{R,A}_+ \otimes \delta\hat{g}^{R,A}\otimes\hat{P}^{R,A}_+ = \hat{0}$ and $\hat{P}^{R,A}_-\otimes\delta\hat{g}^{R,A}\otimes\hat{P}^{R,A}_- = \hat{0}$; as a consequence the spectral response, $\delta\hat{g}^{R,A}$, can be written as

$$\delta\hat{g}^{R,A} = \mp 2\pi i[\hat{P}^{R,A}_+\otimes\delta\hat{X}^{R,A}\otimes\hat{P}^{R,A}_- - \hat{P}^{R,A}_-\otimes\delta\hat{Y}^{R,A}\otimes\hat{P}^{R,A}_+]. \quad \text{(B12)}$$

Analogously, for the anomalous response the normalization condition (37) leads to $\hat{P}^R_+\otimes\delta\hat{g}^a\otimes\hat{P}^A_+ = \hat{0}$ and $\hat{P}^R_-\otimes\delta\hat{g}^a \otimes\hat{P}^A_- = \hat{0}$, so that $\delta\hat{g}^a$ can be written in the following form:

$$\delta\hat{g}^a = -2\pi i[\hat{P}^R_+\otimes\delta\hat{X}^a\otimes\hat{P}^A_- + \hat{P}^R_-\otimes\delta\hat{Y}^a\otimes\hat{P}^A_+]. \quad \text{(B13)}$$

APPENDIX C: PARAMETER REPRESENTATIONS OF THE QUASICLASSICAL GREEN'S FUNCTIONS

The projectors $\hat{P}^R_+$ and $\hat{P}^R_-$ may be parametrized in the following way by complex spin matrices $\gamma^R(\mathbf{p}_f,\mathbf{R},\epsilon,t)$ and $\tilde{\gamma}^R(\mathbf{p}_f,\mathbf{R},\epsilon,t)$:

$$\hat{P}^R_+ = \begin{pmatrix} 1 \\ -\tilde{\gamma}^R \end{pmatrix}\otimes(1-\gamma^R\otimes\tilde{\gamma}^R)^{-1}\otimes(1,\gamma^R), \quad \text{(C1)}$$

$$\hat{P}^R_- = \begin{pmatrix} -\gamma^R \\ 1 \end{pmatrix}\otimes(1-\tilde{\gamma}^R\otimes\gamma^R)^{-1}\otimes(\tilde{\gamma}^R,1). \quad \text{(C2)}$$

Here $(1+a\otimes b)^{-1}$ is defined by

$$(1+a\otimes b)^{-1}\otimes(1+a\otimes b) = 1. \quad \text{(C3)}$$

One immediately proves $\hat{P}^R_+\otimes\hat{P}^R_+ = \hat{P}^R_+$, $\hat{P}^R_-\otimes\hat{P}^R_- = \hat{P}^R_-$ and $\hat{P}^R_+\otimes\hat{P}^R_- = \hat{P}^R_-\otimes\hat{P}^R_+ = \hat{0}$. A useful identity is

$$(1+a\otimes b)^{-1}\otimes a = a\otimes(1+b\otimes a)^{-1}, \quad \text{(C4)}$$

which may be used to obtain $\hat{P}^R_+ + \hat{P}^R_- = 1$. The uniqueness of the projectors is ensured by the symmetry relations between the matrix elements of the retarded and advanced Green's functions. We may obtain the advanced Green's functions either by the fundamental symmetry relation $\hat{g}^A = \hat{\tau}_3(\hat{g}^R)^\dagger\hat{\tau}_3$ or analogously to the retarded case using advanced projectors $\hat{P}^A_+ = \hat{\tau}_3(\hat{P}^R_-)^\dagger\hat{\tau}_3$, $\hat{P}^A_- = \hat{\tau}_3(\hat{P}^R_+)^\dagger\hat{\tau}_3$

$$\hat{P}^A_+ = \begin{pmatrix} -\gamma^A \\ 1 \end{pmatrix}\otimes(1-\tilde{\gamma}^A\otimes\gamma^A)^{-1}\otimes(\tilde{\gamma}^A,1), \quad \text{(C5)}$$

$$\hat{P}^A_- = \begin{pmatrix} 1 \\ -\tilde{\gamma}^A \end{pmatrix}\otimes(1-\gamma^A\otimes\tilde{\gamma}^A)^{-1}\otimes(1,\gamma^A). \quad \text{(C6)}$$

Here $\gamma^A = (\tilde{\gamma}^R)^\dagger$, $\tilde{\gamma}^A = (\gamma^R)^\dagger$ holds. Introducing Eqs. (C1), (C2), (C5), (C6) into Eq. (B6), and using $\epsilon\otimes a + a\otimes\epsilon = 2\epsilon a$ leads to the transport equations for $\gamma^{R,A}$ and $\tilde{\gamma}^{R,A}$, Eqs. (14) and (15), which are generalized Riccati differential equations. They are supplemented by properly chosen initial conditions. The solutions $\tilde{\gamma}^{R,A}$, $\gamma^{R,A}$ are introduced into Eqs. (C1), (C2), (C5), (C6) to obtain the quasiclassical Green's functions, Eqs. (11), (13), via Eq. (B5).

The solutions for the coherence functions in a homogeneous singlet superconductor in equilibrium are

$$\gamma^{R,A}_{\mathrm{hom}} = -\frac{\Delta^{R,A}}{\varepsilon^{R,A} \pm i\sqrt{-\Delta^{R,A}\tilde{\Delta}^{R,A} - (\varepsilon^{R,A})^2}}, \quad \text{(C7)}$$

$$\tilde{\gamma}^{R,A}_{\mathrm{hom}} = \frac{\tilde{\Delta}^{R,A}}{\varepsilon^{R,A} \pm i\sqrt{-\tilde{\Delta}^{R,A}\Delta^{R,A} - (\varepsilon^{R,A})^2}}, \quad \text{(C8)}$$

where $\varepsilon^{R,A} = \epsilon - (\Sigma^{R,A} - \tilde{\Sigma}^{R,A})/2$. Note that $(\Delta^{R,A}\tilde{\Delta}^{R,A})$ is proportional to the unit spin matrix and that in the clean limit $(\Delta^{R,A}\tilde{\Delta}^{R,A}) = -|\Delta|^2$. In the presence of a constant superflow with momentum $\mathbf{p}_s$ one has to make the replacement $\epsilon \rightarrow \epsilon - \mathbf{v}_f\cdot\mathbf{p}_s$.

Using this parametrization the following representation for the Keldysh component with Hermitean spin matrices $x^K(\mathbf{p}_f,\mathbf{R},\epsilon,t)$ and $\tilde{x}^K(\mathbf{p}_f,\mathbf{R},\epsilon,t)$ is convenient. Substituting

$$\hat{X}^K = \begin{pmatrix} x^K & 0 \\ 0 & 0 \end{pmatrix}, \quad \hat{Y}^K = \begin{pmatrix} 0 & 0 \\ 0 & \tilde{x}^K \end{pmatrix}, \quad \text{(C9)}$$

into Eq. (B8), using the equation of motion for $\hat{g}^K$, Eq. (B9), leads to the transport equations for x^K and $\tilde{x}^K$, Eqs. (16) and (17). Note that $\epsilon\otimes a - a\otimes\epsilon = i\hbar\partial_t a$. These transport equations have to be supplemented by initial conditions. For the Keldysh Green's function Eq. (C9) leads to Eq. (12).

It is possible to introduce Shelankov's distribution functions[18] F and $\tilde{F}$, which are given by the parametrization

$$\hat{X}^K=\begin{pmatrix} F & 0 \\ 0 & F \end{pmatrix}, \quad \hat{Y}^K=\begin{pmatrix} \tilde{F} & 0 \\ 0 & \tilde{F} \end{pmatrix}. \tag{C10}$$

They obey the symmetry relations $\tilde{F}(\mathbf{p}_f,\mathbf{R},\epsilon,t)=F(-\mathbf{p}_f,\mathbf{R},-\epsilon,t)^*$, $\tilde{F}(\mathbf{p}_f,\mathbf{R},\epsilon,t)=F(\mathbf{p}_f,\mathbf{R},\epsilon,t)^\dagger$. The x^K and $\tilde{x}^K$ are expressed in terms of them in the following way:

$$x^K=(F-\gamma^R\otimes F\otimes\tilde{\gamma}^A),$$

$$\tilde{x}^K=(\tilde{F}-\tilde{\gamma}^R\otimes\tilde{F}\otimes\gamma^A). \tag{C11}$$

Using the introduced parametrization in terms of coherence functions, the transport equation for F has the form

$$\begin{aligned}&(i\hbar\mathbf{v}_f\boldsymbol{\nabla}F+i\hbar\partial_t F)-\gamma^R\otimes(i\hbar\mathbf{v}_f\boldsymbol{\nabla}F-i\hbar\partial_t F)\otimes\tilde{\gamma}^A\\&\quad+(-\Sigma^R\otimes F+F\otimes\Sigma^A+\Sigma^K)\\&\quad-\gamma^R\otimes(-\tilde{\Sigma}^R\otimes F+F\otimes\tilde{\Sigma}^A-\tilde{\Sigma}^K)\otimes\tilde{\gamma}^A\\&\quad-\gamma^R\otimes(\tilde{\Delta}^R\otimes F-F\otimes\tilde{\Delta}^A+\tilde{\Delta}^K)\\&\quad+(\Delta^R\otimes F-F\otimes\Delta^A-\Delta^K)\otimes\tilde{\gamma}^A=0.\end{aligned} \tag{C12}$$

The transport equation for $\tilde{F}$ follows by application of the conjugation operation, Eq. (10), to this equation. The $\hat{g}^K$ are obtained by introducing Eq. (C11) into Eq. (12). The later parametrization is a convenient starting point for perturbation theory from the equilibrium, because in the equilibrium

$$F_{\mathrm{eq}}=\tanh\frac{\epsilon}{2T}=-\tilde{F}_{\mathrm{eq}}, \tag{C13}$$

holds and all expression in the braces in Eq. (C12) vanish independently.

Finally we make the connection to our parametrization in the linear response. With the choices

$$\delta\hat{X}^{R,A}=\begin{pmatrix} 0 & \delta\gamma^{R,A} \\ 0 & 0 \end{pmatrix}, \quad \delta\hat{Y}^{R,A}=\begin{pmatrix} 0 & 0 \\ \delta\tilde{\gamma}^{R,A} & 0 \end{pmatrix}, \tag{C14}$$

in Eq. (B12), and

$$\delta\hat{X}^a=\begin{pmatrix} \delta x^a & 0 \\ 0 & 0 \end{pmatrix}, \quad \delta\hat{Y}^a=\begin{pmatrix} 0 & 0 \\ 0 & \delta\tilde{x}^a \end{pmatrix}, \tag{C15}$$

in Eq. (B13), we arrive at Eqs. (41)–(48). With this parametrization the linear corrections to the distibution spin matrices $\gamma^{R,A}$, $\tilde{\gamma}^{R,A}$, x^K, $\tilde{x}^K$ are given by $\delta\gamma^{R,A}$, $\delta\tilde{\gamma}^{R,A}$, δx^K, and $\delta\tilde{x}^K$, respectively.

APPENDIX D: REFLECTION AND TRANSMISSION COEFFICENTS

In the superconducting state we define effective reflection and transmission coefficients by

$$\rho_{ij}^R=(1-\gamma_i^R\otimes\tilde{\gamma}_j^R), \quad \tilde{\rho}_{ij}^R=(1-\tilde{\gamma}_i^R\otimes\gamma_j^R), \quad (i,j=1,2), \tag{D1}$$

$$\begin{aligned}R_{1l}^R&=\mathcal{R}\rho_{22}^R\otimes(\mathcal{R}\rho_{22}^R+\mathcal{D}\rho_{12}^R)^{-1},\\ R_{1r}^R&=(\mathcal{R}\tilde{\rho}_{22}^R+\mathcal{D}\tilde{\rho}_{21}^R)^{-1}\otimes\mathcal{R}\tilde{\rho}_{22}^R,\end{aligned} \tag{D2}$$

$$\begin{aligned}\tilde{R}_{1l}^R&=\mathcal{R}\tilde{\rho}_{22}^R\otimes(\mathcal{R}\tilde{\rho}_{22}^R+\mathcal{D}\tilde{\rho}_{12}^R)^{-1},\\ \tilde{R}_{1r}^R&=(\mathcal{R}\rho_{22}^R+\mathcal{D}\rho_{21}^R)^{-1}\otimes\mathcal{R}\rho_{22}^R,\end{aligned} \tag{D3}$$

$$\begin{aligned}A_{1l}^R&=(\gamma_1^R-\gamma_2^R)\otimes(\mathcal{R}\tilde{\rho}_{22}^R+\mathcal{D}\tilde{\rho}_{21}^R)^{-1},\\ A_{1r}^R&=(\mathcal{R}\rho_{22}^R+\mathcal{D}\rho_{12}^R)^{-1}\otimes(\gamma_1^R-\gamma_2^R),\end{aligned} \tag{D4}$$

$$\begin{aligned}\tilde{A}_{1l}^R&=(\tilde{\gamma}_1^R-\tilde{\gamma}_2^R)\otimes(\mathcal{R}\rho_{22}^R+\mathcal{D}\rho_{21}^R)^{-1},\\ \tilde{A}_{1r}^R&=(\mathcal{R}\tilde{\rho}_{22}^R+\mathcal{D}\tilde{\rho}_{12}^R)^{-1}\otimes(\tilde{\gamma}_1^R-\tilde{\gamma}_2^R),\end{aligned} \tag{D5}$$

and $D_{1l}^R=1-R_{1l}^R$, $D_{1r}^R=1-R_{1r}^R$ $\tilde{D}_{1l}^R=1-\tilde{R}_{1l}^R$ $\tilde{D}_{1r}^R=1-\tilde{R}_{1r}^R$. Analogously we define these quantities on the other side of the interface by interchanging 1 and 2. Advanced quantities are given by the same expressions with the change in the superscript $R\to A$. The following relations are shown to hold:

$$A_{1l}^R=\frac{R_{1l}^R}{\mathcal{R}}\otimes\gamma_1^R-\frac{D_{1l}^R}{\mathcal{D}}\otimes\gamma_2^R, \quad A_{1r}^R=\gamma_1^R\otimes\frac{R_{1r}^R}{\mathcal{R}}-\gamma_2^R\otimes\frac{D_{1r}^R}{\mathcal{D}}, \tag{D6}$$

$$\tilde{A}_{1l}^R=\frac{\tilde{R}_{1l}^R}{\mathcal{R}}\otimes\tilde{\gamma}_1^R-\frac{\tilde{D}_{1l}^R}{\mathcal{D}}\otimes\tilde{\gamma}_2^R, \quad \tilde{A}_{1r}^R=\tilde{\gamma}_1^R\otimes\frac{\tilde{R}_{1r}^R}{\mathcal{R}}-\tilde{\gamma}_2^R\otimes\frac{\tilde{D}_{1r}^R}{\mathcal{D}}. \tag{D7}$$

As an example we consider the equilibrium spin-singlet case. In equilibrium the $\otimes$ product reduces to a matrix product. In this case we can write $\gamma^R=i\sigma_y\gamma$, $\tilde{\gamma}^R=i\sigma_y\tilde{\gamma}$, $\Gamma^R=i\sigma_y\Gamma$, $\tilde{\Gamma}^R=i\sigma_y\tilde{\Gamma}$, where γ, $\tilde{\gamma}$, Γ, $\tilde{\Gamma}$ are scalar functions. The effective reflection and transmission coefficients are

$$R_1=\mathcal{R}\frac{1+\gamma_2\tilde{\gamma}_2}{1+\mathcal{R}\gamma_2\tilde{\gamma}_2+\mathcal{D}\gamma_1\tilde{\gamma}_2}, \tag{D8}$$

$$D_1=\mathcal{D}\frac{1+\tilde{\gamma}_2\gamma_1}{1+\mathcal{R}\gamma_2\tilde{\gamma}_2+\mathcal{D}\gamma_1\tilde{\gamma}_2}, \tag{D9}$$

$$\tilde{R}_1=\mathcal{R}\frac{1+\gamma_2\tilde{\gamma}_2}{1+\mathcal{R}\gamma_2\tilde{\gamma}_2+\mathcal{D}\gamma_2\tilde{\gamma}_1}, \tag{D10}$$

$$\tilde{D}_1=\mathcal{D}\frac{1+\gamma_2\tilde{\gamma}_1}{1+\mathcal{R}\gamma_2\tilde{\gamma}_2+\mathcal{D}\gamma_2\tilde{\gamma}_1} \tag{D11}$$

(and analogously for the other side of the interface), which fulfill $R_j+D_j=1$ and $\tilde{R}_j+\tilde{D}_j=1$ $(j=1,2)$.

*Present address: Materials Science Division, Argonne National Laboratory, Argonne, Illinois 60439.

[1] L.D. Landau, Zh. Éksp. Teor. Fiz. **32**, 59 (1957) [Sov. Phys. JETP **5**, 101 (1957)].

[2] G.M. Eliashberg, Zh. Éksp. Teor. Fiz. **42**, 1658 (1962) [Sov. Phys. JETP **15**, 1151 (1962)].

[3] G.M. Eliashberg, Zh. Éksp. Teor. Fiz. **61**, 1254 (1971) [Sov. Phys. JETP **34**, 668 (1972)].

[4] J.W. Serene and D. Rainer, Phys. Rep. **101**, 221 (1983).

[5] A.A. Abrikosov and I.M. Khalatnikov, Rep. Prog. Phys. **22**, 68 (1959).

[6] L.D. Landau, Zh. Éksp. Teor. Fiz. **35**, 97 (1959) [Sov. Phys. JETP **8**, 70 (1959)].

[7] G. Eilenberger, Z. Phys. **214**, 195 (1968).

[8] A.I. Larkin and Y.N. Ovchinnikov, Zh. Éksp. Teor. Fiz. **55**, 2262 (1968) [Sov. Phys. JETP **28**, 1200 (1969)].

[9] J. Bardeen, L.N. Cooper, and J.R. Schrieffer, Phys. Rev. **108**, 1175 (1957).

[10] A.I. Larkin and Y.N. Ovchinnikov, Zh. Éksp. Teor. Fiz. **68**, 1915 (1975) [Sov. Phys. JETP **41**, 960 (1976)]; **73**, 299 (1977) [**46**, 155 (1977)].

[11] L.P. Gor'kov, Zh. Éksp. Teor. Fiz. **34**, 735 (1958) [Sov. Phys. JETP **7**, 505 (1958)]; **36**, 1918 (1959) [**9**, 1364 (1959)].

[12] A.F. Andreev, Zh. Éksp. Teor. Fiz. **46**, 1823 (1964) [Sov. Phys. JETP **19**, 1228 (1964)].

[13] N.N. Bogoliubov, Zh. Éksp. Teor. Fiz. **34**, 58 (1958) [Sov. Phys. JETP **7**, 41 (1958)].

[14] P. G. de Gennes, *Superconductivity in Metals and Alloys* (Benjamin, New York, 1966).

[15] W.J. Tomasch, Phys. Rev. Lett. **15**, 672 (1965); **16**, 16 (1966).

[16] C. Caroli, P.G. de Gennes, and J. Matricon, Phys. Lett. **9**, 307 (1964).

[17] L.V. Keldysh, Zh. Éksp. Teor. Fiz. **47**, 1515 (1964) [Sov. Phys. JETP **20**, 1018 (1965)].

[18] A.L. Shelankov, Zh. Éksp. Teor. Fiz. **78**, 2359 (1980) [Sov. Phys. JETP **51**, 1186 (1980); J. Low Temp. Phys. **60**, 29 (1985).

[19] Y. Nagato, K. Nagai, and J. Hara, J. Low Temp. Phys. **93**, 33 (1993); S. Higashitani and K. Nagai, J. Phys. Soc. Jpn. **64**, 549 (1995); Y. Nagato, S. Higashitani, K. Yamada, and K. Nagai, J. Low Temp. Phys. **103**, 1 (1996).

[20] N. Schopohl and K. Maki, Phys. Rev. B **52**, 490 (1995); N. Schopohl, cond-mat/9804064 (unpublished).

[21] G.E. Blonder, M. Tinkham, and T.M. Klapwijk, Phys. Rev. B **25**, 4515 (1982).

[22] C. Bruder, Phys. Rev. B **41**, 4017 (1990); C. Honerkamp and M. Sigrist, cond-mat/9706199 (unpublished); J. Low Temp. Phys. **111**, 895 (1998).

[23] J. Rammer and H. Smith, Rev. Mod. Phys. **58**, 323 (1986).

[24] A. I. Larkin and Y. N. Ovchinnikov, in *Nonequilibrium Superconductivity*, edited by D. N. Langenberg and A. I. Larkin (Elsevier Science, Amsterdam, 1986), p. 493.

[25] A. A. Abrikosov, L.P. Gor'kov, and I.E. Dzyaloshinski. *Methods of Quantum Field Theory in Statistical Physics* (Prentice-Hall, Englewood Cliffs, NJ, 1963).

[26] M. Eschrig, Ph.D. thesis, Universität Bayreuth, 1997; M. Eschrig, cond-mat/9907312 (unpublished).

[27] A. Schmid and G. Schön, J. Low Temp. Phys. **20**, 207 (1975).

[28] *Nonequilibrium Superconductivity*, edited by A. Schmid in K. E. Gray (Plenum, New York, 1981).

[29] U. Gunsenheimer and A.D. Zaikin, Phys. Rev. B **50**, 6317 (1994); Europhys. Lett. **41**, 195 (1998).

[30] W. Belzig, C. Bruder, and A.L. Fauchère, Phys. Rev. B **58**, 14 531 (1998); A.L. Fauchère, cond-mat/990528 (unpublished); W. Belzig, F.K. Wilhelm, C. Bruder, G. Schön, and A. Zaikin, cond-mat/9812297 (unpublished); Superlattices Microstruct. **25**, 1251 (1999).

[31] A.V. Zaitsev, Zh. Éksp. Teor. Fiz. **86**, 1742 (1984) [Sov. Phys. JETP **59**, 1015 (1984)]; A.L. Shelankov, Fiz. Tverd. Tela (Leningrad) **26**, 1615 (1984) [Sov. Phys. Solid State **26**, 981 (1984)].

[32] A. Millis, D. Rainer, and J.A. Sauls, Phys. Rev. B **38**, 4504 (1988).

[33] B. Ashauer, G. Kieselmann, and D. Rainer, J. Low Temp. Phys. **63**, 349 (1986).

[34] G. Kieselmann, Phys. Rev. B **35**, 6762 (1987).

[35] K. Nagai and J. Hara, J. Low Temp. Phys. **71**, 351 (1988); M. Ashida, S. Aoyoma, J. Hara, and K. Nagai, Phys. Rev. B **40**, 8673 (1989).

[36] S.-K. Yip, J. Low Temp. Phys. **109**, 547 (1997).

[37] The second equalities in Eqs. (32) and (33) can be verified using relations such as $(\mathcal{D}\gamma_1^R+\mathcal{R}\gamma_2^R)\otimes[1-\tilde{\gamma}_2^R\otimes(\mathcal{D}\gamma_1^R+\mathcal{R}\gamma_2^R)]^{-1}$ $=[1-(\mathcal{D}\gamma_1^R+\mathcal{R}\gamma_2^R)\otimes\tilde{\gamma}_2^R]^{-1}\otimes(\mathcal{D}\gamma_1^R+\mathcal{R}\gamma_2^R)$.

[38] M. Eschrig, cond-mat/9804330 (unpublished); M. Eschrig, J.A. Sauls, and D. Rainer, cond-mat/9805299 (unpublished); M. Eschrig, J. A. Sauls, and D. Rainer, Phys. Rev. B **60**, 10 447 (1999). In order to generalize the formulation to the full spin space we changed slightly our notation compared to Refs. 26 and 38. The connection to the equations in these references is made by the following replacements in the current paper: $\gamma^{R,A}\rightarrow\pm i\sigma_y\gamma^{R,A}$, $\tilde{\gamma}^{R,A}\rightarrow\pm i\sigma_y\tilde{\gamma}^{R,A}$, and analog replacements for $\Delta^{R,A}$, $\tilde{\Delta}^{R,A}$ and all the corresponding linear response quantities.

[39] D.J. Van Harlingen, Rev. Mod. Phys. **67**, 515 (1995); D.J. Scalapino, Phys. Rep. **250**, 329 (1995).

[40] L. Buchholtz and G. Zwicknagl, Phys. Rev. B **23**, 5788 (1981).

[41] C.R. Hu, Phys. Rev. Lett. **72**, 1526 (1994); C. Yang and C.R. Hu, Phys. Rev. B **50**, 16 766 (1994).

[42] M. Matsumoto and H. Shiba, J. Phys. Soc. Jpn. **64**, 3384 (1995); **64**, 4867 (1995).

[43] Y. Tanaka and S. Kashiwaya, Phys. Rev. Lett. **74**, 3451 (1995); Phys. Rev. B **53**, 9371 (1996).

[44] M. Fogelström, D. Rainer, and J.A. Sauls, Phys. Rev. Lett. **79**, 281 (1997); M. Covington, M. Aprili, E. Paraoanu, L.H. Greene, F. Xu, J. Zhu, and C.A. Mirkin, *ibid.* **79**, 277 (1997); **79**, 2598 (1997); D. Rainer, H. Burkhardt, M. Fogelström, and J.A. Sauls, J. Phys. Chem. Solids **59**, 2040 (1998).

[45] L. Alff, H. Takashima, S. Kashiwaya, N. Terada, H. Hara, Y. Tanaka, M. Koyanagi, and K. Kajimura, Phys. Rev. B **55**, R14 757 (1997); L. Alff, S. Kleefisch, U. Schoop, M. Zittartz, T. Kemen, T. Bauch, A. Marx and R. Gross, cond-mat/9806150 (unpublished).

[46] R. Meservey and P.M. Tedrow, Phys. Rep. **238**, 173 (1994).

[47] G. Kieselmann and D. Rainer, Z. Phys. B: Condens. Matter **52**, 267 (1983).

[48] S.-K. Yip, Phys. Rev. B **32**, 2915 (1985).

[49] W. Zhang, J. Kurkijärvi, D. Rainer, and E.V. Thuneberg, Phys. Rev. B **37**, 3336 (1988).

[50] J. Kurkijärvi and D. Rainer, in *Helium Three*, edited by W. P. Halperin and L. P. Pitaevskij (Elsevier Science Publishers, British Vancouver, 1990), pp. 313-325.

[51] T. Tokuyasu, J.A. Sauls, and D. Rainer, Phys. Rev. B **38**, 8823 (1988).

[52] A.L. Shelankov, Fiz. Tverd. Tela (Leningrad) **26**, 1615 (1984)

[Sov. Phys. Solid State **26**, 981 (1984)].
[53] M.F. Atiyah, V.K. Patodi, and I.M. Singer, Math. Proc. Cambridge. Philos. Soc. **77**, 43 (1975).
[54] M. Sigrist, D.B. Bailey, and R.B. Laughlin, Phys. Rev. Lett. **74**, 3249 (1995).
[55] L.J. Buchholtz, M. Palumbo, D. Rainer, and J.A. Sauls, J. Low Temp. Phys. **101**, 1079 (1995); **101**, 1099 (1995).
[56] M. Palumbo, P. Muzikar, and J.A. Sauls, Phys. Rev. B **42**, 2681 (1990).